

AD-A184 886

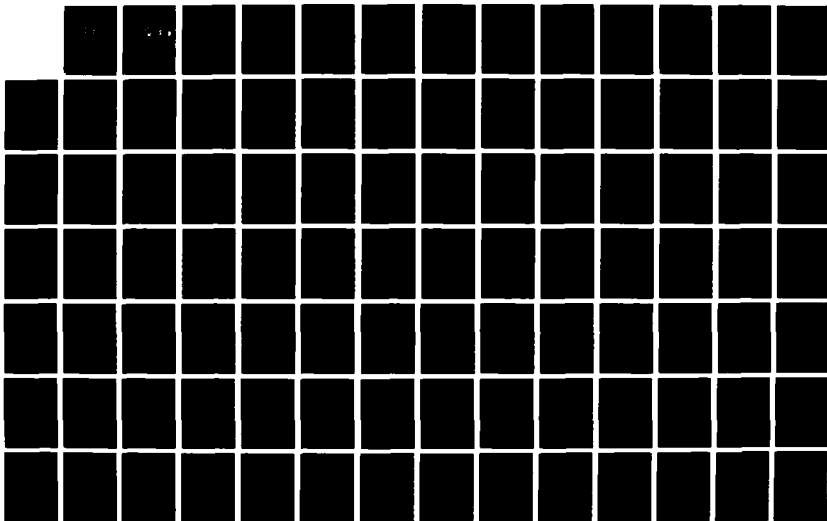
PROPERTIES OF THE ATMOSPHERIC BOUNDARY LAYER ABOVE A  
SUBTROPICAL OCEANIC FRONT(U) NAVAL POSTGRADUATE SCHOOL  
MONTEREY CA J P HIGGINS JUN 87

1/2

UNCLASSIFIED

F/G 4/2

NL





AD-A184 006

DTIC FILE COPY

2

# NAVAL POSTGRADUATE SCHOOL

Monterey, California



DTIC  
ELECTE  
SEP 03 1987  
S D  
CLD

## THESIS

PROPERTIES OF THE ATMOSPHERIC BOUNDARY  
LAYER ABOVE A SUBTROPICAL  
OCEANIC FRONT



by

John P. Higgins

JUNE 1987

Thesis Advisor

K. L. Davidson

Approved for public release; distribution is unlimited.

87 9 1 318

UNCLASSIFIED

SECURITY CLASSIFICATION OF THIS PAGE

## REPORT DOCUMENTATION PAGE

1a REPORT SECURITY CLASSIFICATION UNCLASSIFIED			1b RESTRICTIVE MARKINGS		
2a SECURITY CLASSIFICATION AUTHORITY			3 DISTRIBUTION/AVAILABILITY OF REPORT		
2b DECLASSIFICATION/DOWNGRADING SCHEDULE			Approved for public release; Distribution unlimited.		
4 PERFORMING ORGANIZATION REPORT NUMBER(S)			5 MONITORING ORGANIZATION REPORT NUMBER(S)		
6a NAME OF PERFORMING ORGANIZATION Naval Postgraduate School		6b OFFICE SYMBOL (if applicable) 63	7a NAME OF MONITORING ORGANIZATION Naval Postgraduate School		
6c ADDRESS (City, State, and ZIP Code) Monterey, California 93943-5000			7b ADDRESS (City, State, and ZIP Code) Monterey, California 93943-5000		
8a NAME OF FUNDING/SPONSORING ORGANIZATION		8b OFFICE SYMBOL (if applicable)	9 PROCUREMENT INSTRUMENT IDENTIFICATION NUMBER		
8c ADDRESS (City, State, and ZIP Code)			10 SOURCE OF FUNDING NUMBERS		
			PROGRAM ELEMENT NO	PROJECT NO	TASK NO
			WORK UNIT ACCESSION NO		
11 TITLE (Include Security Classification) PROPERTIES OF THE ATMOSPHERIC BOUNDARY LAYER ABOVE A SUBTROPICAL OCEANIC FRONT					
12 PERSONAL AUTHOR(S) Higgins, John P.					
13a TYPE OF REPORT Master's Thesis		13b TIME COVERED FROM _____ TO _____		14 DATE OF REPORT (Year, Month, Day) 1987 June	
15 PAGE COUNT 99					
16 SUPPLEMENTARY NOTATION					
17 COSATI CODES			18 SUBJECT TERMS (Continue on reverse if necessary and identify by block number)		
FIELD	GROUP	SUB-GROUP	Atmospheric Boundary Layer, FASINEX, Sub-Tropical Western Atlantic.		
19 ABSTRACT (Continue on reverse if necessary and identify by block number) The marine atmospheric boundary layer (MABL) and synoptic-scale situation is described using rawinsonde and sea-surface temperature (SST) data collected during the 1986 Frontal Air-Sea Interaction Experiment (FASINEX). The data obtained from 14 February to 09 March 1986 are divided into eight consecutive three-day periods and analyzed. Significant changes in synoptic-scale features and flow patterns occurred during each three-day period due to movement of low pressure systems. MABL changes noted were due primarily to large scale convergence. Thirteen pairs of rawinsonde launches, seven from opposite sides of an oceanic front and six from the same side (five warm, one cold) are compared. The time difference between soundings in each pair did not exceed sixty minutes. Boundary layer height, mixed layer potential temperature and specific humidity differences between paired rawinsonde launches were larger when launches were from					
20 DISTRIBUTION/AVAILABILITY OF ABSTRACT <input checked="" type="checkbox"/> UNCLASSIFIED/UNLIMITED <input type="checkbox"/> SAME AS RPT <input type="checkbox"/> DTIC USERS			21 ABSTRACT SECURITY CLASSIFICATION UNCLASSIFIED		
22a NAME OF RESPONSIBLE INDIVIDUAL Prof. K.L. Davidson			22b TELEPHONE (Include Area Code) (408) 646-2309		22c OFFICE SYMBOL 63Ds

DD FORM 1473, 84 MAR

83 APR edition may be used until exhausted  
All other editions are obsolete

SECURITY CLASSIFICATION OF THIS PAGE

UNCLASSIFIED

SECURITY CLASSIFICATION OF THIS PAGE (When Data Entered)

# 19 (cont.)

opposite sides of the oceanic front. A combination of both shipboard and aircraft data will be necessary to further describe the conditions of the MABL and synoptic-scale situation.

S N 0102- LF-014-6601

UNCLASSIFIED

2

SECURITY CLASSIFICATION OF THIS PAGE (When Data Entered)

Approved for public release; distribution is unlimited.

Properties of the Atmospheric Boundary Layer Above a Subtropical  
Oceanic Front

by

John P. Higgins  
Lieutenant, United States Navy  
B.S., Northeastern University, 1976

Submitted in partial fulfillment of the  
requirements for the degree of

MASTER OF SCIENCE IN METEOROLOGY AND OCEANOGRAPHY


from the


NAVAL POSTGRADUATE SCHOOL  
JUNE 1987

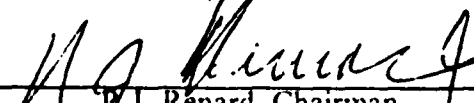
Author:

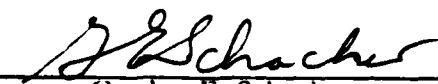
  
John P. Higgins

Approved by:

  
K.L. Davidson, Thesis Advisor

  
W.J. Shaw, Second Reader

  
R.J. Renard, Chairman,  
Department of meteorology

  
Gordon E. Schacher,  
Dean of Science and Engineering

## ABSTRACT

➤The marine atmospheric boundary layer (MABL) and synoptic-scale situation is described using rawinsonde and sea-surface temperature (SST) data collected during the 1986 Frontal Air-Sea Interaction Experiment (FASINEX). The data obtained from 14 February to 09 March 1986 are divided into eight consecutive three-day periods and analyzed. Significant changes in synoptic-scale features and flow patterns occurred during each three-day period due to movement of low pressure systems. MABL changes noted were due primarily to large scale convergence. Thirteen pairs of rawinsonde launches, seven from opposite sides of an oceanic front and six from the same side (five warm, one cold) are compared. The time difference between soundings in each pair did not exceed sixty minutes. Boundary layer height, mixed layer potential temperature and specific humidity differences between paired rawinsonde launches were larger when launches were from opposite sides of the oceanic front. A combination of both shipboard and aircraft data will be necessary to further describe the conditions of the MABL and synoptic-scale situation,

## TABLE OF CONTENTS

I.	INTRODUCTION.....	11
II.	FASINEX DATA.....	15
	A. INTRODUCTION .....	15
	B. RAWINSONDE MEASUREMENTS.....	16
III.	RESULTS.....	23
	A. SYNOPTIC-SCALE CONDITIONS AND MABL CHANGES.....	23
	1. 14 February - 16 February 1986.....	24
	2. 17 February - 19 February 1986.....	30
	3. 20 February - 22 February 1986.....	36
	4. 23 February - 25 February 1986.....	41
	5. 26 February - 28 February 1986.....	47
	6. 01 March - 03 March 1986.....	53
	7. 04 March - 06 March 1986.....	58
	8. 07 March - 09 March 1986.....	64
	B. PROFILE PROPERTIES.....	70
IV.	SUMMARY AND CONCLUSIONS.....	93
	LIST OF REFERENCES.....	96
	INITIAL DISTRIBUTION LIST.....	97



Accession For	
NTIS CRA&I	<input checked="" type="checkbox"/>
DTIC TAB	<input type="checkbox"/>
Unannounced	<input type="checkbox"/>
Justification	
By	
Date	
Distribution	
Dist	
A-1	



## LIST OF TABLES

I.	RAWINSONDE FLIGHTS.....	18
II.	RAWINSONDE SENSOR SPECIFICATIONS.....	22
III.	RAWINSONDE SOUNDING PAIRS.....	72

## LIST OF FIGURES

1.1	Frontal Air-Sea Interaction Experiment (FASINEX) area .....	14
3.1	Surface Weather Map, 14 - 16 Feb. 1986 .....	25
3.2	Time Series 14 Feb. - 16 Feb. 1986 .....	26
3.3	Radiosonde Profiles, 14 Feb. 86 (top), 15 Feb. 86 (mid), 16 Feb. 86 (bot) .....	28
3.4	Surface Weather Map, 17 Feb. - 19 Feb. 1986 .....	31
3.5	Time Series 17 Feb. - 19 Feb. 1986 .....	32
3.6	Radiosonde Profiles, 17 Feb. 86 (top), 18 Feb. 86 (mid), 19 Feb. 86 (bot) .....	34
3.7	Surface Weather Map, 20 Feb. - 22 Feb. 1986 .....	37
3.8	Time Series 20 Feb. - 22 Feb. 1986 .....	38
3.9	Radiosonde Profiles, 20 Feb. 86 (top), 21 Feb. 86 (mid), 22 Feb. 86 (bot) .....	40
3.10	Surface Weather Map, 23 Feb. - 25 Feb. 1986 .....	43
3.11	Time Series 23 Feb. - 25 Feb. 1986 .....	44
3.12	Radiosonde Profiles, 23 Feb. 86 (top), 24 Feb. 86 (mid), 25 Feb. 86 (bot) .....	45
3.13	Surface Weather Map, 26 Feb. - 28 Feb. 1986 .....	48
3.14	Time Series 26 Feb. - 28 Feb. 1986 .....	50
3.15	Radiosonde Profiles, 26 Feb. 86 (top), 27 Feb. 86 (mid), 28 Feb. 86 (bot) .....	51
3.16	Surface Weather Map, 01 Mar. - 03 Mar. 1986 .....	54
3.17	Time Series 01 Mar. - 03 Mar. 1986 .....	55
3.18	Radiosonde Profiles, 01 Mar. 86 (top), 02 Mar. 86 (mid), 03 Mar. 86 (bot) .....	56
3.19	Surface Weather Map, 04 Mar. - 06 Mar. 1986 .....	59
3.20	Time Series 04 Mar. - 06 Mar. 1986 .....	60
3.21	Radiosonde Profiles, 04 Mar. 86 (top), 05 Mar. 86 (mid), 06 Mar. 86 (bot) .....	62
3.22	Surface Weather Map, 07 Mar. - 09 Mar. 1986 .....	65

3.23	Time Series 07 Mar. - 09 Mar. 1986 .....	66
3.24	Radiosonde Profiles, 07 Mar. 86 (top), 08 Mar. 86 (mid), 09 Mar. 86 (bot) .....	68
3.25	Radiosonde Profile Comparison ENDEAVOR 17 Feb. 86, 2352 GMT, 28 18N, 70 25W, cold side (thin), OCEANUS 18 Feb. 86, 0049 GMT, 28 02N, 70 05W, warm side (thick) .....	73
3.26	Radiosonde Profile Comparison ENDEAVOR 18 Feb. 86, 1459 GMT, 28 28N, 70 29W, cold side (thin), OCEANUS 18 Feb. 86, 1525 GMT, 28 04N, 70 15W, warm side (thick) .....	75
3.27	Radiosonde Profile Comparison ENDEAVOR 21 Feb. 86, 1952 GMT, 28 12N, 70 03W, warm side (thin), OCEANUS 21 Feb. 86, 1915 GMT, 28 59N, 69 56W, cold side (thick) .....	77
3.28	Radiosonde Profile Comparison ENDEAVOR 05 Mar. 86, 0616 GMT, 28 53N, 67 52W, cold side (thin), OCEANUS 05 Mar. 86, 0542 GMT, 28 46, 68 03W, warm side (thick) .....	78
3.29	Radiosonde Profile Comparison ENDEAVOR 05 Mar. 86, 2054 GMT, 28 45N, 67 47W, warm side (thin), OCEANUS 05 Mar. 86, 1952 GMT, 29 14N, 67 50W, cold side (thick) .....	80
3.30	Radiosonde Profile Comparison ENDEAVOR 06 Mar. 86, 1226 GMT, 28 50N, 67 36W, cold side (thin), OCEANUS 06 Mar. 86, 1151 GMT, 27 17N, 69 17W, warm side (thick) .....	81
3.31	Radiosonde Profile Comparison ENDEAVOR 07 Mar. 86, 0014 GMT, 28 36N, 67 18W, cold side (thin), OCEANUS 07 Mar. 86, 0011 GMT, 27 08N, 69 34W, warm side (thick) .....	83
3.32	Radiosonde Profile Comparison ENDEAVOR 22 Feb. 86, 1919 GMT, 28 18N, 69 20W, warm side (thin), OCEANUS 22 Feb. 86, 1825 GMT, 28 13N, 69 48W, warm side (thick) .....	85
3.33	Radiosonde Profile Comparison ENDEAVOR 24 Feb. 86, 1413 GMT, 27 56N, 69 49W, warm side (thin), OCEANUS 24 Feb. 86, 1358 GMT, 28 14N, 69 40W, warm side (thick) .....	86
3.34	Radiosonde Profile Comparison ENDEAVOR 27 Feb. 86, 2357 GMT, 27 10N, 69 48W, warm side (thin), OCEANUS 28 Feb. 86, 0016 GMT, 28 42N, 70 08W, warm side (thick) .....	88
3.35	Radiosonde Profile Comparison ENDEAVOR 05 Mar. 86, 0014 GMT, 28 30N, 68 03W, warm side (thin), OCEANUS 04 Mar. 86, 2348 GMT, 28 33N, 68 08W, warm side (thick) .....	89
3.36	Radiosonde Profile Comparison ENDEAVOR 07 Mar. 86, 0606 GMT, 28 50N, 67 28W, warm side (thin), OCEANUS 07 Mar. 86, 0551 GMT, 26 54N, 70 02W, warm side (thick) .....	90

3.37	Radiosonde Profile Comparison ENDEAVOR 19 Feb. 86, 1200	
	GMT, 28 47N, 70 11W, cold side (thin), OCEANUS 19 Feb. 86, 1215	
	GMT, 28 49N, 70 34W , cold side (thick) .....	91

#### ACKNOWLEDGEMENTS

I personally wish to thank:

- Professor K.L. Davidson for his professional guidance and assistance in completing this thesis;
- Professor W.J. Shaw for his review and constructive criticism;
- Pat J. Boyle, Sheryl Fellbaum, Tamar Neta and Shirley Duff for their continuous help, patience and constructive criticism.

Very special thanks to my wife, Lisa, for her strength and love that made it all worthwhile.

## I. INTRODUCTION

The marine atmospheric boundary layer (MABL) is that region above the surface layer directly affected by the exchange between the underlying ocean and the overlying atmosphere. A predominant feature of the marine atmospheric boundary layer is the existence of temperature and humidity gradients at the top of a well mixed layer. This layer is cool and moist relative to the overlying air and is observed to have depths ranging from 100 to 1000 m over the eastern North Pacific Ocean and from 1000 to 2000 m in the more subtropical waters.

Recent studies provide quite good descriptions of physical properties and processes responsible for MABL features which enable interpretation of observed data. General features of the MABL with regard to surface conditions have been reviewed by Businger (1985). Observed MABL features across an ocean thermal front were described by Hsu et al. (1985). MABL features associated with forced convection and large scale subsidence have been described by Davidson et al. (1984). Businger and Shaw (1984) described the effects of sea-surface temperature variation on the turbulence regime which controls MABL mixing and entrainment processes. Wyngaard and Brost (1983) presented a physical model for gradients within the well mixed portion of the MABL.

The MABL has several unique characteristics caused by the underlying water surface. Marine air, being moist, often has a slightly unstable stratification. Additionally, the sea-surface temperature is uniform with horizontal variations seldom exceeding several degrees Celsius over a distance of 50 km, so differential advection has a meaningful role in the MABL formation. The height of the MABL is partially controlled by thermal forcing. Due to the unstable surface layer, turbulent kinetic energy is transported upward by buoyant thermals. The impingement on the inversion by these eddies entrains overlying air so that in the absence of subsidence, the inversion height will rise. Turbulence caused by radiational cooling of the cloud tops is also suggested as a cause of entrainment at the top of the mixed layer.

The Department of Defense is interested in understanding processes and events occurring within and at the top of the MABL. For example, gradients in the MABL affect electromagnetic (EM) and electro-optical (EO) systems. Refraction at layers where large temperature and humidity gradients exist leads to ducting of EM waves. Turbulence causes small scale inhomogeneities in the index of refraction which is important in image resolution at EO wave lengths. Aerosol and water vapor in the MABL are also important in extinction of EO waves.

Data for this thesis were collected in the Frontal Air-Sea Interaction Experiment (FASINEX), which was partially sponsored by the Office of Naval Research, during the period 13 February - 10 March 1986. FASINEX was a multi-group experiment designed to further investigate the role of horizontal temperature variabilities in air-sea interaction. FASINEX was conducted in the subtropical convergence zone of the North Atlantic Ocean south of Bermuda (within the area bounded by 62°W and 72°W and by 26°N and 30°N). See Fig. 1.1. This region was chosen for FASINEX due to the common presence of well defined oceanic fronts. Oceanic fronts are relatively long lived and have surface temperature gradients up to  $0.40^{\circ}\text{C km}^{-1}$  (Weller and Stage, 1984). The field work was centered on an area spanning an oceanic front.

Scientific goals of FASINEX addressed the following questions (Stage and Weller, 1985 and Weller and Stage, 1984): Does the strong horizontal gradient in sea-surface temperature associated with the oceanic front affect the structure of the marine atmospheric boundary layer? Do the fluxes of momentum, heat and moisture in the lower atmosphere vary horizontally on scales determined by the scales of the oceanic front? Does the response of the upper ocean to atmospheric forcing vary on scales determined by the oceanic front as well as by the atmosphere? Are there atmospheric and oceanic boundary layers in the region around the oceanic front?



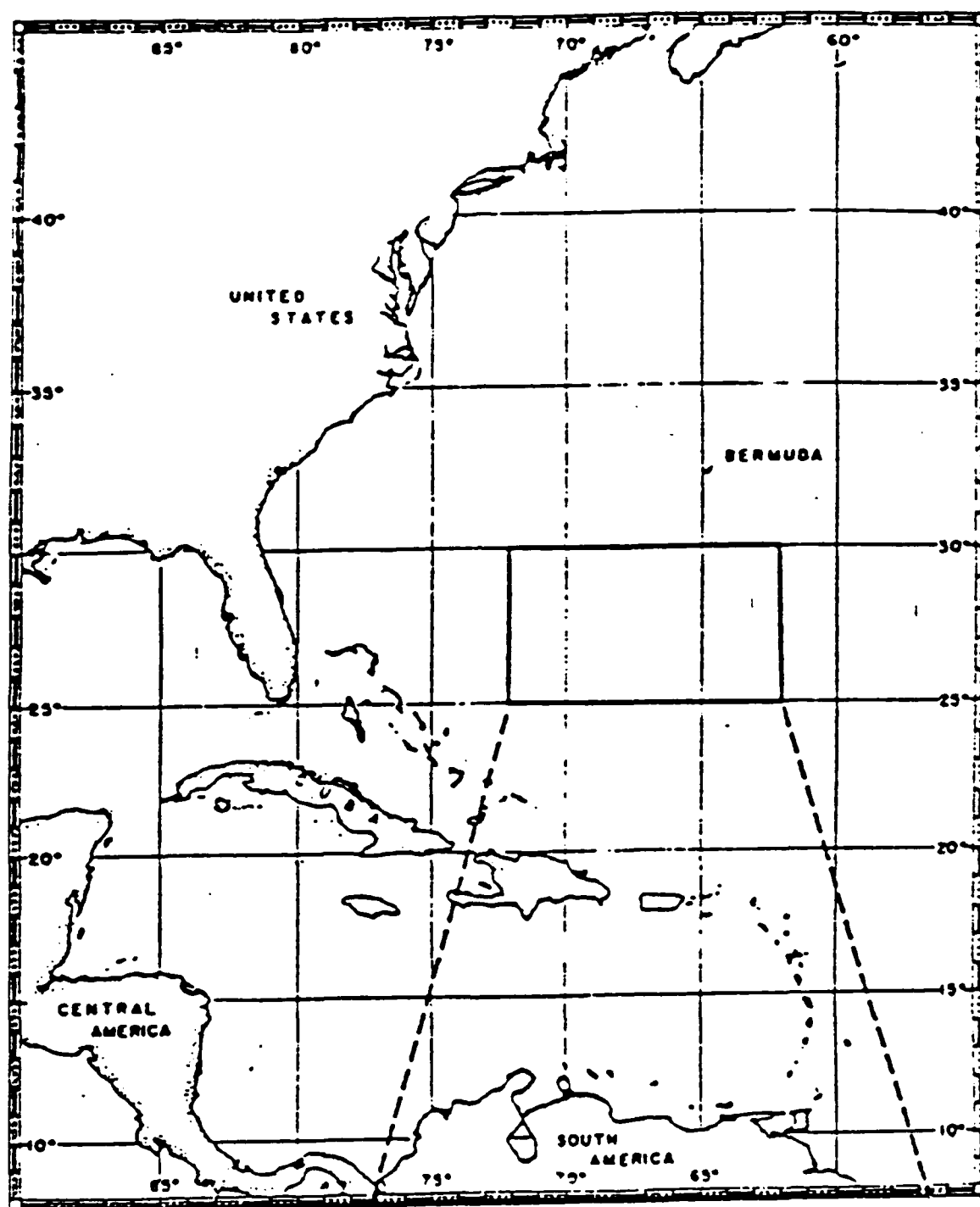


Figure 1.1 Frontal Air-Sea Interaction Experiment (FASINEX) area.

The purposes of this thesis will be to describe features of the MABL with regard to synoptic-scale conditions and with regard to the sea-surface temperature fronts, and to present physical reasons for the observed variations. The descriptions will include the synoptic-scale, surface layer and mixed layer conditions which occurred.

## II. FASINEX DATA

### A. INTRODUCTION

Meteorological data in FASINEX were collected by satellite remote sensing, moored buoy arrays, surface ships and aircraft. This thesis will describe results from the surface ship data collection only.

The FASINEX shipboard meteorological program focused on the vertical and horizontal structure of the surface layer and MABL with respect to oceanic sea-surface temperature fronts and coupled oceanic and atmospheric mixed layers. Measurements were made from two ships, the R/V OCEANUS and the R/V ENDEAVOR, and consisted of surface layer mean and turbulent wind, air temperature and humidity. MABL measurements consisted of inversion heights, temperature, humidity and wind profiles, based on rawinsondes.

Aircraft measurements provided horizontal variation of turbulence intensities at fixed levels (Stage and Weller, 1985). Ship measurements provided surface layer values for the horizontal variation of turbulence intensities and were closely correlated to changes in surface boundary thermal

conditions. The small scale turbulence intensity values from all sources are necessary to assess MABL growth due to entrainment.

The FASINEX oceanography program was extensive and, for this thesis, provided information on sea-surface temperature patterns and frontal locations. The R/V OCEANUS was the platform used to make surveys of the front on the basis of 80-km-long sections across it. The R/V OCEANUS also was located in and near the front for short periods. The R/V ENDEAVOR was the platform used to investigate small scale structure found in the vicinity of the front and more detailed velocity/density sections across the front. Hence, the R/V ENDEAVOR was mostly in the frontal region.

#### B. RAWINSONDE MEASUREMENTS

Rawinsondes were a primary method of data collection because they provide vertical measurements of wind as well as vertical distribution of temperature and humidity. Two VIZ Inc. WL-8000 RPT systems, one each aboard the R/V's ENDEAVOR and OCEANUS, were used to obtain atmospheric dynamic and thermodynamic profiles from rawinsonde launches. These systems yielded pressure, temperature, humidity and vector wind profiles, typically up to 7.5-9.5 km (400-300 mb). The systems sampled all five variables every fifteen seconds which provided vertical resolutions of 35 to 50 m from balloon ascent rates averaging  $2.5-3.2 \text{ ms}^{-1}$ .

Two to four rawinsonde launches were made daily from both the R/V's ENDEAVOR and OCEANUS. The positions, dates and times of all such sonde flights are tabulated and presented in Table 1. During the period from 13 February to 7 March, a total of 70 launches were attempted from the ENDEAVOR with 58 successful for both wind and thermodynamic profiles, and 64 with satisfactory thermodynamic profiles. Of the 64 ENDEAVOR flights with usable thermodynamic data, only six did not have wind information. 96 launches were attempted from the OCEANUS between 13 February and 10 March, with 68 successful thermodynamic soundings. Unfortunately, adopted launch techniques for the OCEANUS prohibit useful wind data at this time.

Each rawinsonde is individually factory calibrated, with met-sensor calibration results displayed on a bar-code affixed to every sonde casement. A bar-wand records the calibration values into a WL-8000RPT microprocessor prior to each launch. These are ultimately used by the computer reduction software to generate the finished thermodynamic data. Pertinent rawinsonde sensor specifications, as given by the manufacturer are listed in Table 2.

Wind speeds and directions are derived from the VIZ sondes using LORAN-C navigational aids. The VIZ sensor package receives LORAN time differences to establish position. The filtered data are differentiated with respect to time to obtain balloon velocity. It is assumed that the

TABLE I  
RAWINSONDE FLIGHTS

DATE	TIME	SHIP	LOCATION	
			WEST	NORTH
860213	1204	ENDEAVOR	69 59.13	28 11.22
	1714	OCEANUS	68 01.47	29 59.32
	1845	ENDEAVOR	70 09.01	27 42.26
860214	0018	ENDEAVOR	70 30.05	28 04.67
	1245	ENDEAVOR	71 00.10	28 08.30
	1500	ENDEAVOR	70 58.32	28 17.96
	1502	OCEANUS	69 35.13	27 53.93
	2345	ENDEAVOR	70 45.57	27 52.99
860215	0545	OCEANUS	70 02.09	26 38.35
	1207	ENDEAVOR	70 28.31	28 03.75
	1800	ENDEAVOR	70 28.51	28 12.38
860216	0043	ENDEAVOR	70 14.29	28 08.03
	0603	ENDEAVOR	70 27.01	28 14.38
	0731	OCEANUS	70 17.38	27 57.80
	1259	ENDEAVOR	70 28.07	28 07.39
	1933	OCEANUS	69 35.54	27 56.54
	2358	ENDEAVOR	70 28.94	28 13.86
	2358	OCEANUS	69 37.66	27 24.04
860217	0607	OCEANUS	69 45.21	28 05.03
	1213	ENDEAVOR	70 31.88	28 06.13
	1804	ENDEAVOR	70 29.00	28 04.26
	2352	ENDEAVOR	70 25.58	28 18.42
860218	0049	OCEANUS	70 05.40	28 02.81
	0548	OCEANUS	70 05.72	28 41.39
	1200	ENDEAVOR	70 27.71	28 22.99
	1459	ENDEAVOR	70 29.03	28 28.41
	1521	OCEANUS	70 15.38	28 04.59
	1826	ENDEAVOR	70 25.88	28 35.92
860219	0000	ENDEAVOR	70 27.97	28 33.97
	0603	OCEANUS	69 32.79	27 59.76
	1200	ENDEAVOR	70 11.01	28 45.57
	1215	OCEANUS	70 34.58	28 49.43
	1757	ENDEAVOR	70 23.53	28 27.37
	2027	OCEANUS	70 44.21	28 02.86
	2334	OCEANUS	70 42.87	28 28.46

TABLE 1 CONT.

DATE	TIME	SHIP	LOCATION	
			WEST	NORTH
860220	0645	OCEANUS	70 06.81	28 33.56
	1211	ENDEAVOR	70 07.10	28 29.11
	1441	OCEANUS	70 04.78	28 13.83
	1507	ENDEAVOR	69 57.75	28 50.05
	1854	ENDEAVOR	69 53.08	28 49.00
	2023	OCEANUS	69 59.12	28 12.43
860221	0052	ENDEAVOR	69 56.15	28 08.54
	1210	ENDEAVOR	69 51.76	28 13.52
	1515	OCEANUS	69 55.77	28 52.87
	1915	OCEANUS	69 56.80	28 59.45
	1952	ENDEAVOR	70 02.33	28 11.17
860222	0000	ENDEAVOR	70 08.87	28 16.42
	0612	OCEANUS	69 26.19	28 10.94
	1201	ENDEAVOR	68 53.62	28 30.80
	1825	OCEANUS	69 47.84	28 13.19
	1919	ENDEAVOR	69 19.65	28 18.03
860223	0000	ENDEAVOR	69 23.01	28 23.11
	0608	OCEANUS	69 43.86	28 11.17
	1209	ENDEAVOR	69 38.11	28 02.33
	2027	ENDEAVOR	69 41.65	28 02.23
860224	0001	ENDEAVOR	69 39.06	28 01.19
	0545	OCEANUS	69 28.86	28 10.58
	1358	OCEANUS	69 40.73	28 14.46
	1413	ENDEAVOR	69 48.43	27 55.41
	1832	ENDEAVOR	69 47.29	27 52.28
	2020	OCEANUS	69 35.10	28 15.82
	2356	ENDEAVOR	69 24.61	28 03.90
860225	0601	OCEANUS	69 24.55	28 10.97
	1230	ENDEAVOR	69 35.23	28 29.52
	1343	ENDEAVOR	69 38.81	28 27.29
	1759	ENDEAVOR	69 36.40	28 22.79
	2233	OCEANUS	69 21.94	28 16.19
860226	0008	ENDEAVOR	69 12.83	28 11.75
	1159	ENDEAVOR	69 23.00	28 15.21
	1402	OCEANUS	69 16.18	27 59.98
	1825	OCEANUS	69 28.38	27 40.36
	2306	ENDEAVOR	69 43.86	27 27.35

TABLE 1 CONT.

DATE	TIME	SHIP	LOCATION	
			WEST	NORTH
860227	0315	ENDEAVOR	69 43.94	27 09.06
	0557	OCEANUS	69 48.25	26 35.02
	1213	ENDEAVOR	69 48.66	26 55.91
	1926	ENDEAVOR	69 50.62	27 00.17
	2357	ENDEAVOR	69 48.58	27 09.05
860228	0016	OCEANUS	70 08.60	28 41.90
	0549	OCEANUS	69 22.59	28 49.08
	1156	OCEANUS	68 25.05	28 48.61
	1400	ENDEAVOR	68 41.87	28 10.54
	1748	OCEANUS	68 24.42	28 06.24
	2351	ENDEAVOR	68 31.40	28 32.70
860301	0554	OCEANUS	69 15.22	28 21.31
	1414	ENDEAVOR	68 23.59	28 22.91
860302	0008	ENDEAVOR	68 24.54	28 07.01
	0554	OCEANUS	68 24.66	28 58.81
	1449	ENDEAVOR	68 53.95	28 08.76
	1806	ENDEAVOR	69 02.73	28 10.55
860303	0010	ENDEAVOR	69 04.83	28 12.56
	0558	OCEANUS	68 34.18	28 46.45
	1157	ENDEAVOR	68 26.10	28 46.70
	1500	ENDEAVOR	68 28.22	28 57.64
	2054	ENDEAVOR	68 27.82	28 38.64
	2210	OCEANUS	68 34.80	28 37.87
	2359	ENDEAVOR	68 29.85	28 57.48
860304	0557	OCEANUS	68 14.71	28 36.52
	1114	ENDEAVOR	67 57.68	28 48.56
	1156	ENDEAVOR	67 59.86	28 44.93
	1310	ENDEAVOR	68 01.15	28 38.68
	1926	OCEANUS	68 14.29	28 23.36
	2348	OCEANUS	68 08.31	28 33.42
860305	0014	ENDEAVOR	68 03.02	28 29.44
	0542	OCEANUS	68 03.56	28 46.17
	0616	ENDEAVOR	67 51.10	28 53.00
	0952	OCEANUS	67 57.23	28 54.86
	1331	OCEANUS	67 54.77	29 00.13
	1952	OCEANUS	67 50.41	29 14.12
	2054	ENDEAVOR	67 46.56	28 42.65

TABLE 1 CONT.

DATE	TIME	SHIP	LOCATION	
			WEST	NORTH
860306	0005	ENDEAVOR	67 39.44	28 50.14
	0602	OCEANUS	68 34.00	28 06.60
	1151	OCEANUS	69 17.30	27 17.70
	1226	ENDEAVOR	67 35.44	28 48.04
	1757	OCEANUS	69 46.84	27 05.61
	2001	ENDEAVOR	67 30.19	28 42.00
860307	0011	OCEANUS	69 33.98	27 08.04
	0014	ENDEAVOR	67 17.67	28 34.83
	0551	OCEANUS	70 02.76	26 54.31
	0606	ENDEAVOR	67 27.18	28 49.12
	1346	OCEANUS	69 33.96	27 18 29
	1609	OCEANUS	69 34.04	27 00.52
	1807	OCEANUS	69 43.73	26 54.14
	2026	OCEANUS	70 02.42	26 54.08
860308	0025	OCEANUS	70 02.06	27 22.57
	1216	OCEANUS	69 51.21	26 27.90
	1756	OCEANUS	70 05.57	26 54.97
	2358	OCEANUS	69 50.37	27 07.88
860309	0637	OCEANUS	69 33.79	27 22.50
	1223	OCEANUS	69 39.60	28 19.90
	1849	OCEANUS	69 43.72	29 40.40
860310	0036	OCEANUS	69 49.57	30 57.14
	0612	OCEANUS	69 56.28	32 10.46
	1144	OCEANUS	70 04.25	33 21.84
	1740	OCEANUS	70 16.51	34 38.44



TABLE II

RAWINSONDE SENSOR SPECIFICATIONS  
(VIZ SONDE MODEL #1523)

VARIABLE	SENSOR	RANGE	ACCURACY
Pressure	Aneroid Capsule Ni-Span-C)	1080-5 mb	+ 2 mb
Temperature	Rod-Type Thermistor	50°-90° c	+ 0.4° c
Relative Humidity	Carbon Resistance Element (Fast Response)	5-100% 40+0° -60° c	+ 4%
Wind Vector	Loran-C Nav aids	N/A	+ 0.5 m/s + 2° c

horizontal velocity of the balloon and local mean wind velocity are the same. It is noted that the best vector wind accuracies apply to conditions which produce LORAN signals at (near perpendicular) crossing angles in the time difference isopleths of two LORAN secondary stations. More than 80% of the total wind soundings in FASINEX fell within the ranges  $+0.5-2 \text{ ms}^{-1}$  and  $+2-10^{\circ}\text{C}$ . The higher limits were due to weak LORAN signals, an expected result since the FASINEX survey area was on the fringe of coverage of the U.S. LORAN southeast chain (GRI 7980) (COMDTINST M16562.3).

### III. RESULTS

#### A. SYNOPTIC-SCALE CONDITIONS AND MABL CHANGES

The MABL is significantly modulated by atmospheric synoptic-scale conditions. Surface layer stability, synoptic-scale subsidence and clouds also affect the height of the mixed layer. Wind speed affects mechanical mixing and the air/sea temperature differences affect the stability and thermal mixing. Frontal passages provide a good opportunity to observe the MABL under rapidly changing synoptic-scale conditions.

The above factors indicate the importance of this section which will include detailed descriptions of the synoptic-scale features and associated mixed layers. The synoptic-scale variations in FASINEX were significant because of the high frequency of frontal passages (every

three to five days). The discussion of synoptic-scale features will be divided into eight three-day subsections. The meteorological data used are from the R/V ENDEAVOR unless otherwise indicated.

In this section, mixed layer changes will be related to changes in synoptic-scale conditions indicating low-level flow and upper-level divergence or convergence.

1. 14 February - 16 February 1986

This was a period of changing synoptic-scale conditions. As shown in Fig. 3.1, the beginning of the period was dominated by a high pressure system, while the end of the period was dominated by an approaching low pressure system with a frontal passage shortly after 0000 GMT 16 February.

On 14 February, the subtropical high pressure center redeveloped after being disrupted by a cold front on the previous day (Fig. 3.1). Sea-level pressures increased from 1021-1026 mb as the system moved eastward towards the FASINEX area. Wind speeds decreased from  $12 \text{ ms}^{-1}$  to  $5 \text{ ms}^{-1}$  and wind direction shifted from northwest to northeast. An unstable air-sea temperature difference of  $5^{\circ}\text{C}$  was recorded (Fig. 3.2). Fig. 3.2 shows a three-day time series of temperature (sea-dotted, air solid), relative humidity, pressure, true wind speed and direction, and relative wind speed and direction. Dominant cloud types were stratocumulus, altostratus and cirrus. The top of the mixed

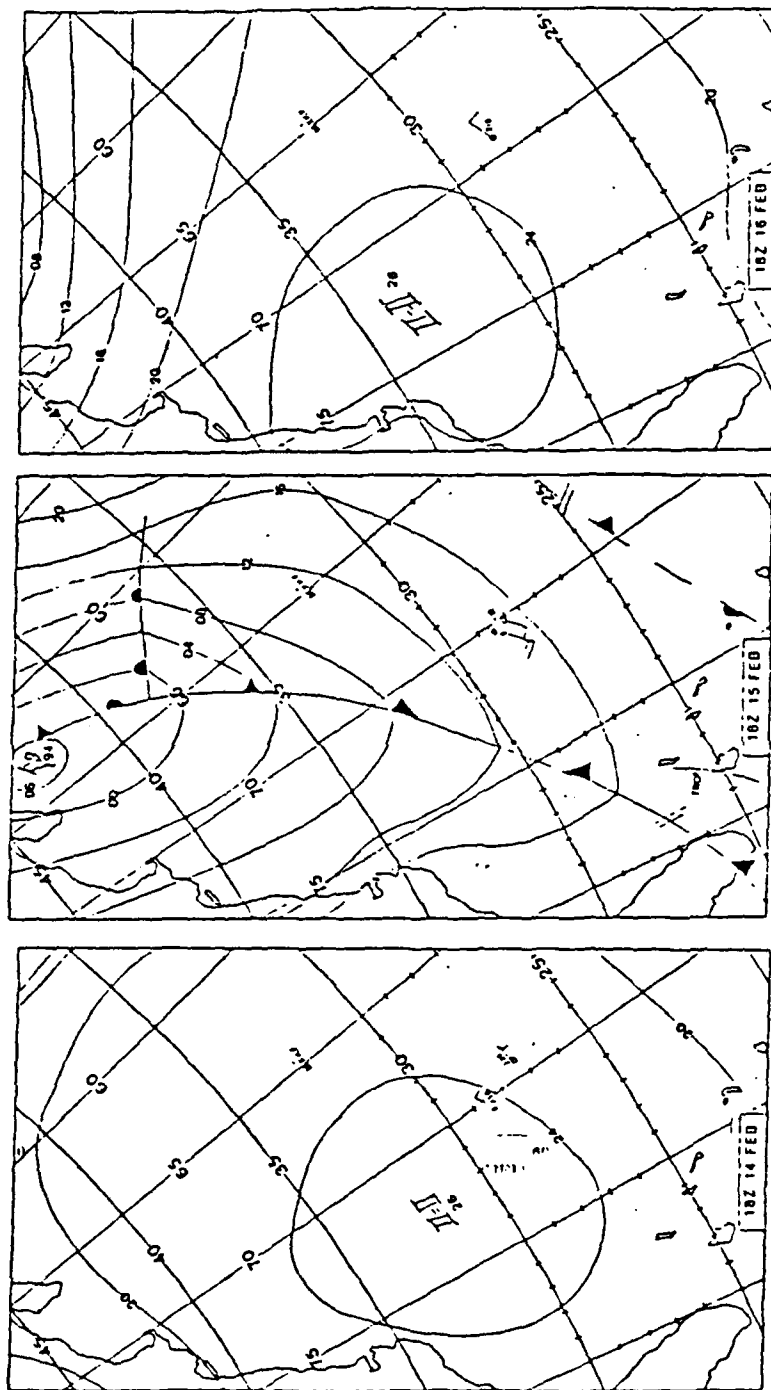


Figure 3.1 Surface Weather Map, 14 - 16 Feb. 1986.

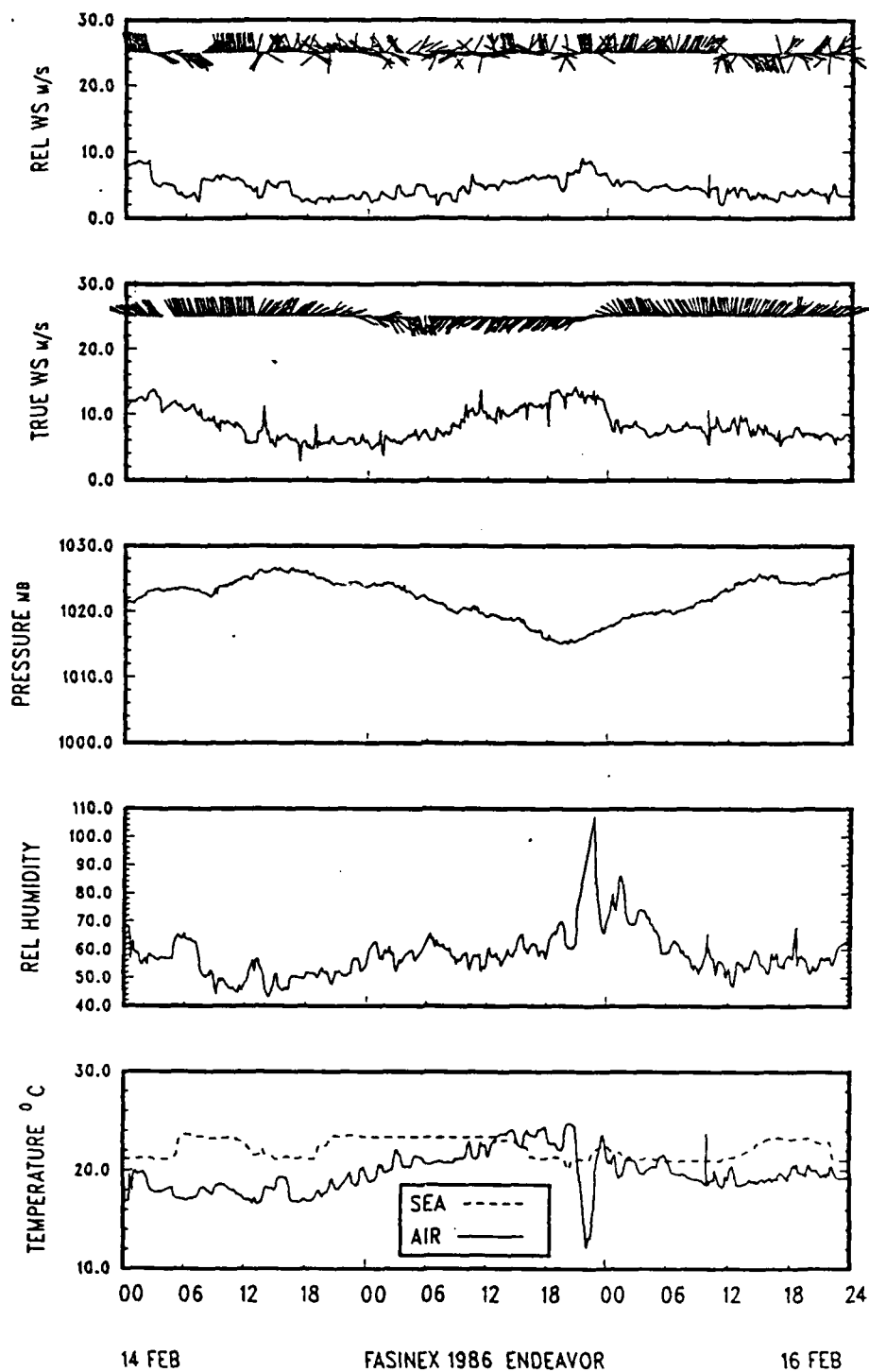


Figure 3.2 Time Series 14 Feb. - 16 Feb. 1986.

layer was slightly above 1500 m and potential temperature and specific humidity within it were well mixed (Fig. 3.3). Fig. 3.3 represents a three-day time series of rawinsonde profiles taken aboard the ENDEAVOR. Both potential temperature and specific humidity are shown as well as the vertical distribution of wind speed and direction. No precipitation was recorded on this date.

The high moved northeastward on 15 February and a deepening upper-level trough (500 mb) and an associated sea-level low pressure system began to affect conditions by 1000 GMT (Fig. 3.1), causing the sea-level pressure to drop. The wind speed increased and the wind direction shifted to the southeast. Sea-level pressure dropped to 1013 mb and wind speed increased to  $14 \text{ ms}^{-1}$  by 2000 GMT. Wind direction shifted to the southeast by 1200 GMT. An unstable air-sea temperature difference of  $1-4^{\circ}\text{C}$  existed until 1200 GMT when warm air over the cooler frontal sea surface caused a stable condition until 2000 GMT. At 2000 GMT a sharp drop in air temperature accompanied by a sharp increase in relative humidity occurred (Fig. 3.2). Temperature and humidity conditions similar to those before 2000 GMT had returned by 2300 GMT. Cloud cover consisted of lower to mid-level stratus, stratocumulus and altostratus. Partial clearing occurred at 1200 GMT. Mixed layer height was 1500 m and both potential temperature and specific humidity remained well mixed below the inversion (Fig. 3.3). Precipitation in

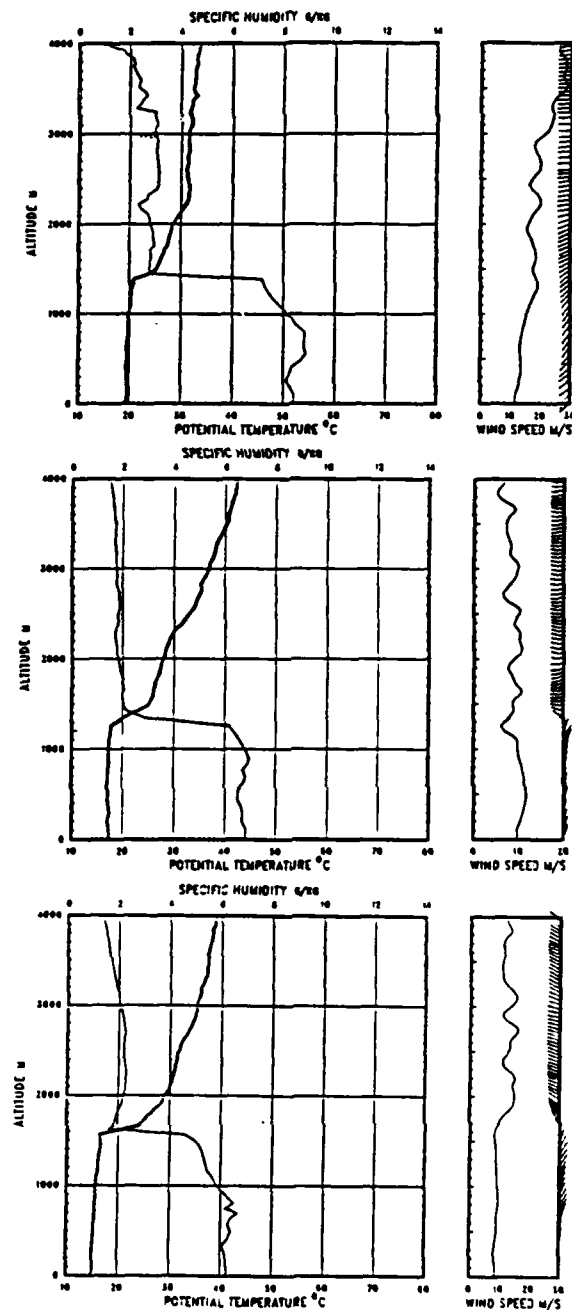


Figure 3.3 Radiosonde Profiles, 14 Feb. 86 (top),  
15 Feb. 86 (mid), 16 Feb. 86 (bot).

the form of rain showers occurred at 0000 GMT on 16 February.

On 16 February the cold front and the upper-level trough passed through the FASINEX area at 0000 GMT (Fig. 3.1). The sea-level pressure increased steadily to a maximum of 1026 mb (8 mb rise) by 0000 GMT on 17 February. Wind speed dropped rapidly after the frontal passage to a minimum of  $6 \text{ ms}^{-1}$ . The wind direction shifted from southwest to northwest with the frontal passage and then shifted to the northeast (1600 GMT) as a high began to dominate the synoptic-scale conditions (Fig. 3.1). An unstable air-sea temperature difference of  $1\text{-}3^{\circ}\text{C}$  existed until 0000 GMT on 17 February (Fig. 3.2). Cloud cover was mostly low-level stratus and stratocumulus. Rain showers occurred from 0000-0100 GMT. The mixed layer height was approximately 1300 m and potential temperature and specific humidity below the inversion were well mixed (Fig. 3.3).

This period illustrates the role of the synoptic-scale conditions, relative to flow, on the vertical profiles of the MABL. Mixed layer feature evolution over these three days, as shown in Fig. 3.3, reflected the upwind sea-level properties very distinctly. On the 14th and 16th the upwind sea-level temperatures were cooler due to the northerly flow. The mixed layer potential temperatures were between  $15$  and  $17^{\circ}\text{C}$  and the specific humidities were between 6 and  $8 \text{ gkg}^{-1}$ . On the 15th the upwind sea-level temperatures were



higher due to southwest flow and the mixed layer temperature was 20°C and the mixed layer humidity was above 8 gkg<sup>-1</sup>.

The mixed layer depth was about the same, within 200 m, on all three days. In fact, they were closer on the 15th and 16th even though the 15th launch was in advance of an approaching front and the launches on the 14th and 16th were in nearly identical locations in the sea-level high pressure system. The similarity also exists in the vector wind profiles from the sea-level through the inversion and in the temperature and humidity values above the inversion.

## 2. 17 February - 19 February 1986

The first two days of this period were dominated by a high pressure system shown in Fig. 3.4. On 19 February synoptic-scale conditions began to show characteristic pre-frontal movement patterns.

The upper-level winds returned to a zonal pattern on 17 February and the high pressure system dominated the synoptic-scale conditions into the following day (Fig. 3.4). Sea-level pressure was steady ranging from 1024-1026 mb. Wind speed was steady at 6-8 ms<sup>-1</sup> but the wind direction shifted from northeast to southeast as the center of the high moved northeastward. An unstable air-sea temperature difference of 1-3°C remained until 1200 GMT (Fig. 3.5). Stratus and stratocumulus cloud cover increased during the day. Small amounts of high cirrus were also present. The mixed layer height increased from 1000 to 2000 m between the

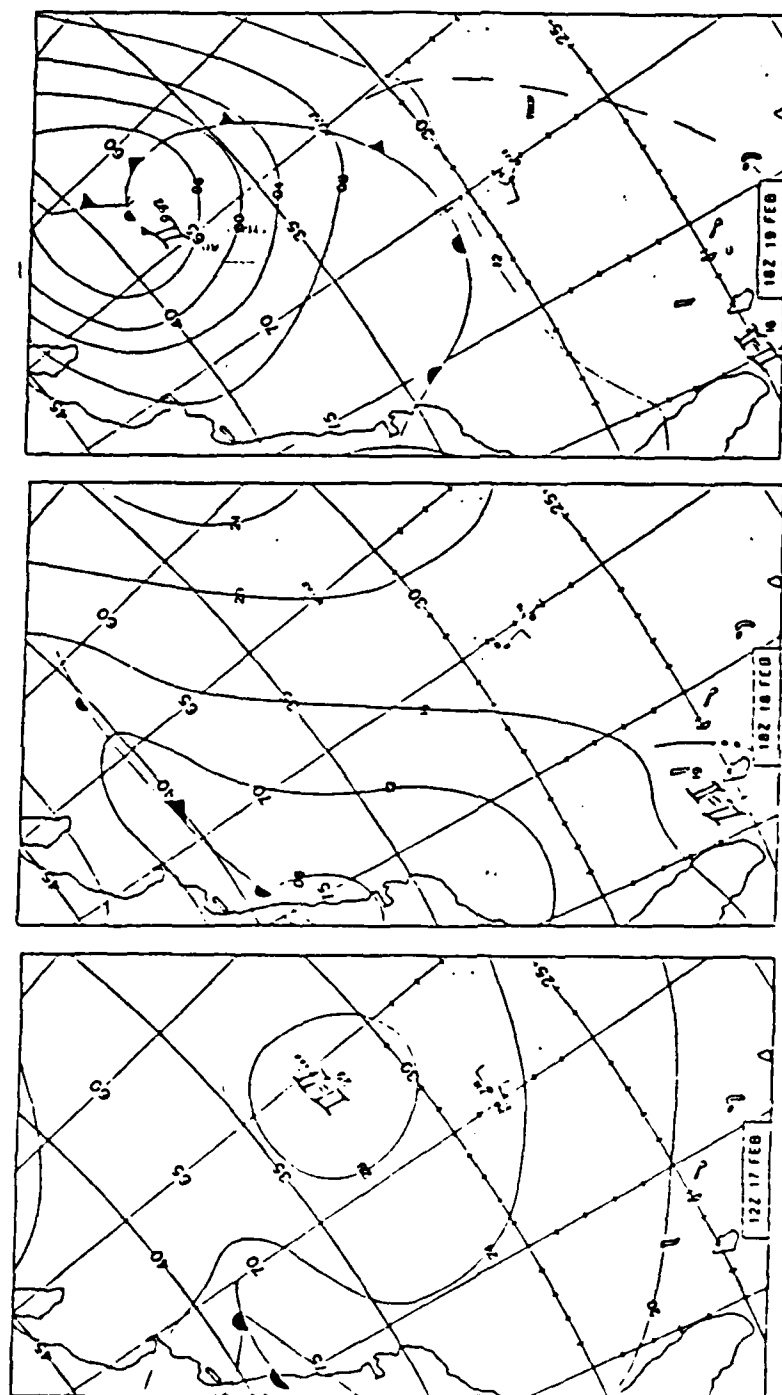


Figure 3.4 Surface Weather Map, 17 Feb. - 19 Feb. 1986.

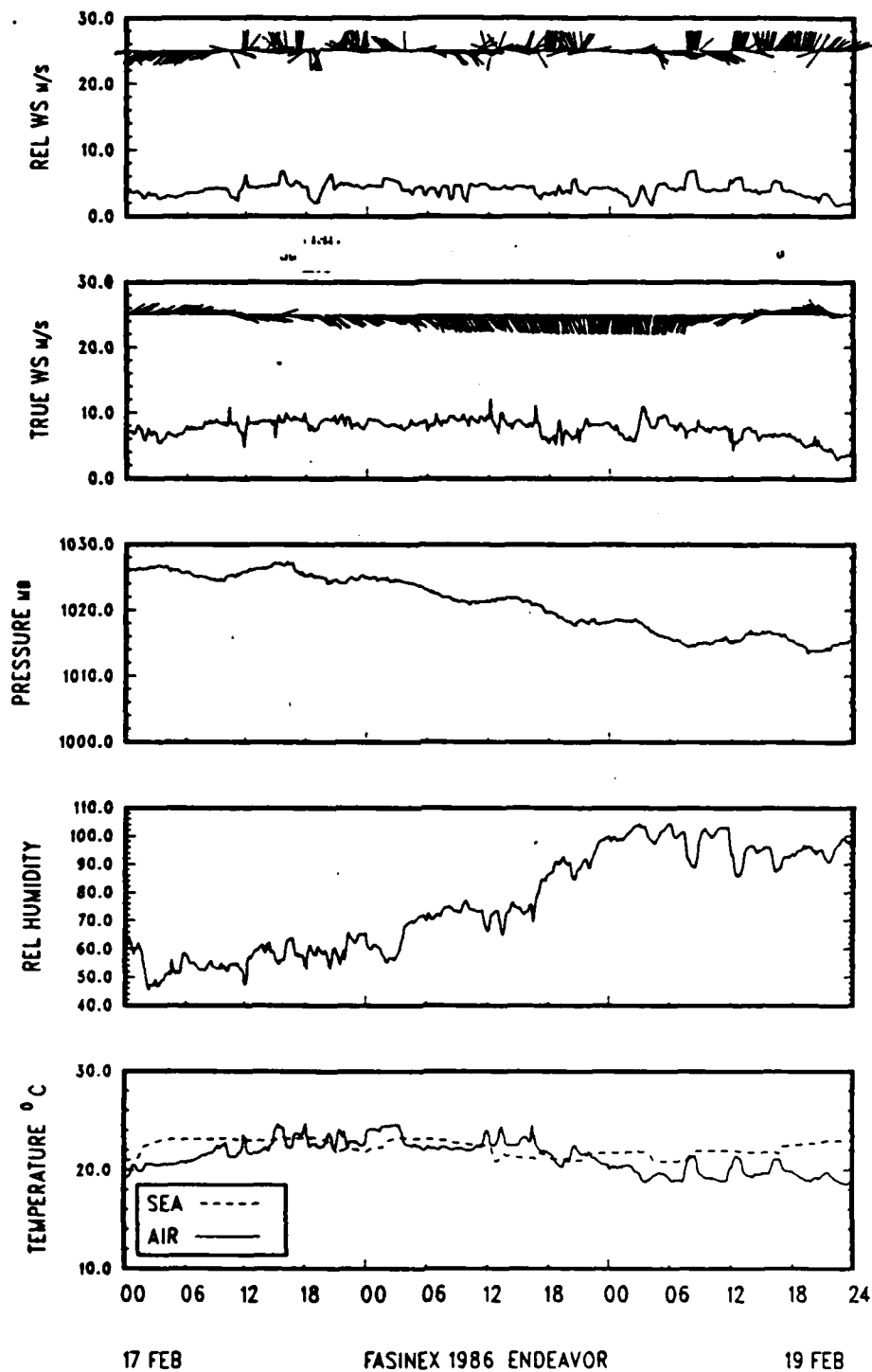


Figure 3.5 Time Series 17 Feb. - 19 Feb. 1986.

16th and 17th. Potential temperature and specific humidity remained well mixed below the inversion (Fig. 3.6).

The upper-level winds developed a ridge pattern as the sea-level high intensified to the north of the FASINEX region on 18 February (Fig. 3.4). Sea-level pressure decreased steadily (4mb) as the center of the high moved northeastward. Wind speed and direction were steady at 6-8  $\text{ms}^{-1}$  from the southeast. A slightly stable air-sea temperature difference of  $2^{\circ}\text{C}$  existed until 0500 GMT when the ENDEAVOR crossed the sea surface temperature (SST) front causing a  $1^{\circ}\text{C}$  unstable condition until 1200 GMT (Fig. 3.5). From 1200 to 1800 GMT conditions once again became stable. Unstable conditions returned by 2000 GMT and continued into the following day. Low to mid-level stratus clouds were present with rain showers taking place from 1800-0000 GMT. Mixed layer height was 800 m (Fig. 3.6).

On 19 February an upper-level trough and a sea-level low pressure system moved off the east coast of the United States and began affecting conditions by 1200 GMT (Fig. 3.4). Sea-level pressure decreased steadily to 1015 mb. Wind speed ranged from 4-6  $\text{ms}^{-1}$  and wind direction shifted from south to southwest as the cold front approached (1200 GMT). By 1600 GMT the frontal system began moving northward causing the wind to shift to the northwest. An unstable air-sea temperature difference of  $1-5^{\circ}\text{C}$  was present until 0000 GMT on 20 February (Fig. 3.5). Cloud cover

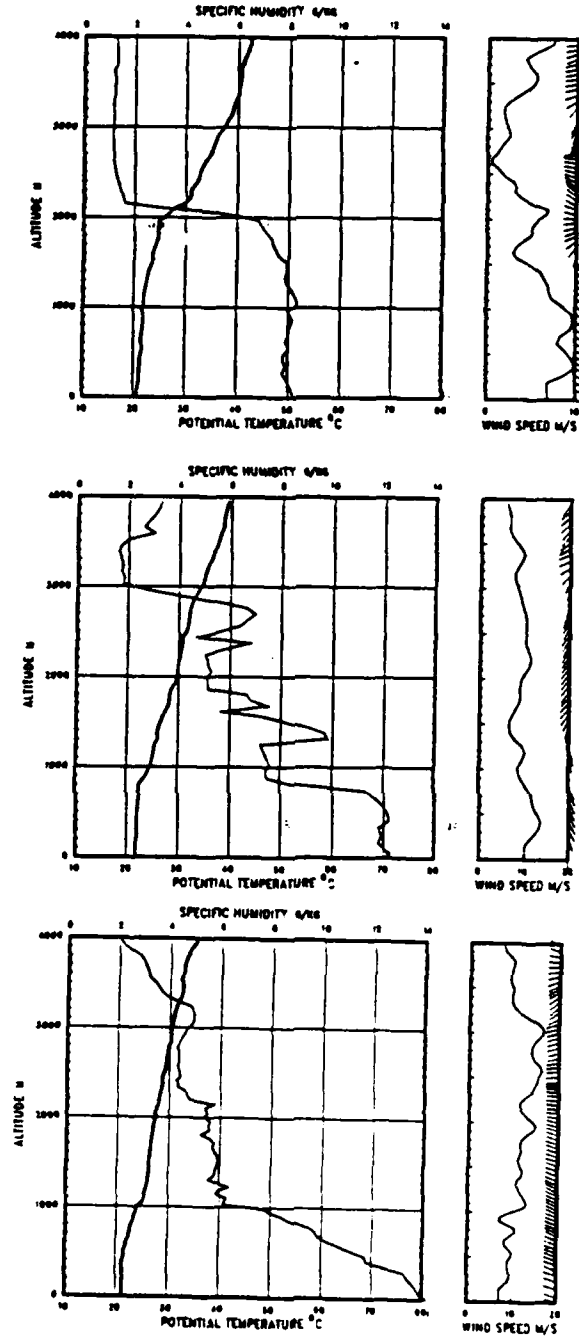


Figure 3.6 Radiosonde Profiles, 17 Feb. 86 (top),  
18 Feb. 86 (mid), 19 Feb. 86 (bot).

consisted of low and mid-level stratus with small amounts of cirrus present. Rain showers occurred at 0500 GMT and light showers at 1100 GMT. The mixed layer height was close to 500 m (Fig. 3.6).

The response to the synoptic-scale circulation is quite evident during this period. Easterly flow, over warmer water, under the influence of a northeastward retracting high pressure system caused an increase on the 17th of the mixed layer specific humidity to  $8 \text{ gkg}^{-1}$  from below  $7 \text{ gkg}^{-1}$  on the 16th and an increase of the mixed layer height, due to decreased subsidence, to 2000 m from 1300 m on the 16th.

On the 18th, as the FASINEX area became less influenced by the high, the inversion at 2000 m became less distinct. The convergence associated with the approaching trough caused the moisture to be lifted to 3000 m. However, southerly flow with upwind warmer water caused a mixed layer of 900 m to form in the FASINEX area with much higher specific humidities,  $12 \text{ gkg}^{-1}$ . The wind profiles above 1300 m look quite similar on the 17th and 18th indicating the mixed layer was the only region affected between the two days.

On the 19th, the trough passage seems to have had an effect at levels above 1000 m. Below 1000 m, the westerly flow caused continued high values of mixed layer specific humidity. A distinct mixed layer with clouds, from

300-1000 m, existed. The increase of specific humidity from 12 to above 14 gkg<sup>-1</sup> is viewed to be significant since the shift of wind was from southeast to westerly flow.

### 3. 20 February - 22 February 1986

This period showed a general change in the synoptic-scale situation. The first day of the period was influenced by a low pressure system. By the middle of this period a weak sea-level high pressure system began to develop and was dominating synoptic-scale conditions until the end of the period.

The upper-level trough stalled on 20 February allowing a weak cold front to rapidly pass through the FASINEX region (Fig. 3.7). Frontal passage, based on the wind shift conditions, occurred at 1500 GMT. Sea-level pressure dropped to 1008 mb (8 mb drop), wind speed increased from 4-10 ms<sup>-1</sup> and the wind direction shifted from southwest to northwest after the frontal passage. An unstable air-sea temperature difference of 4-8°C was present until 1800 GMT (frontal passage), when warm air advected over the cooler water yielding a stable condition until 0000 GMT (Fig. 3.8). Cloud cover consisted of mid-level stratus with small amounts of cirrus and occasional clearing. Rain occurred at 0700 GMT and a strong thunderstorm (heavy rain, lightning, strong winds) occurred from 1735-1740 GMT. A waterspout was reported by aircraft. The mixed layer height was 750 m with potential temperature being well mixed and

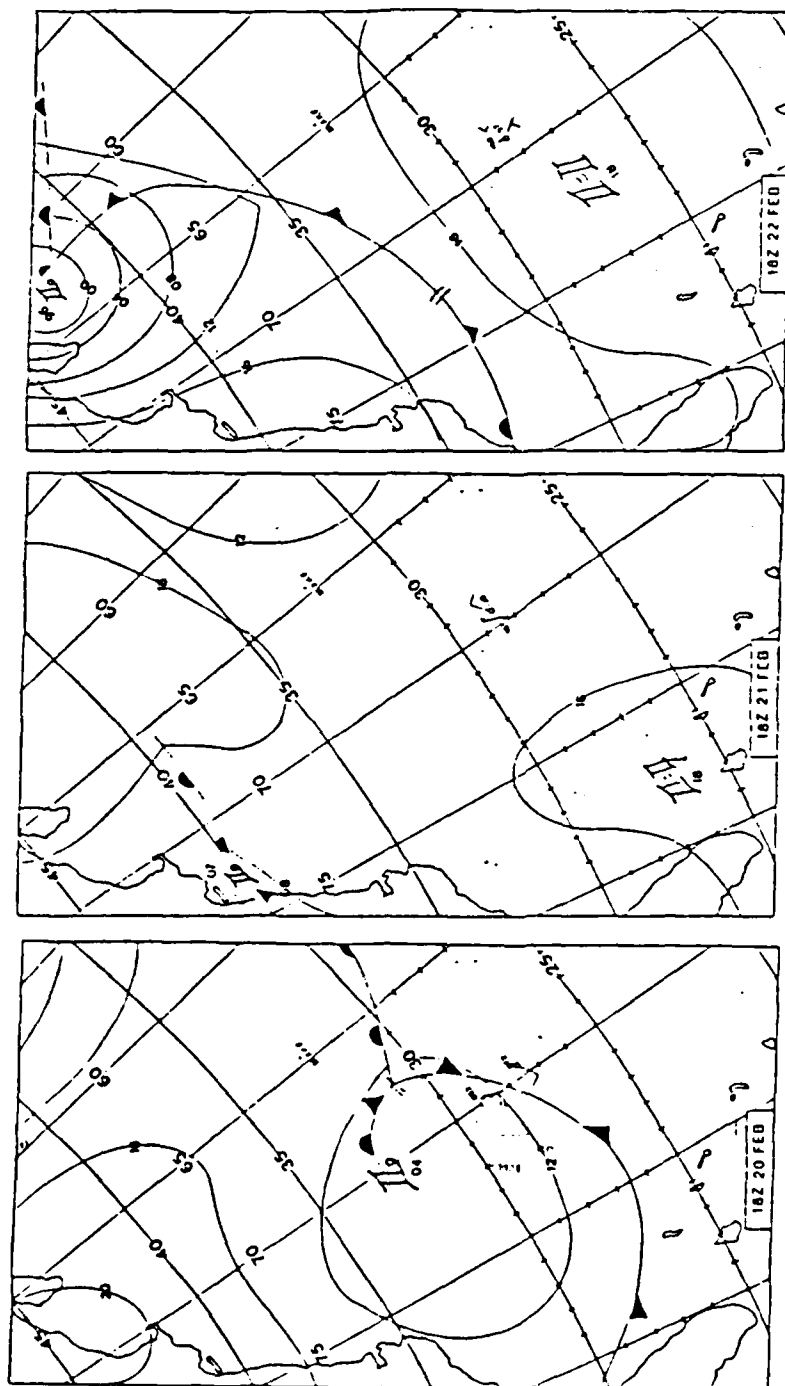


Figure 3.7 Surface Weather Map, 20 Feb. - 22 Feb. 1986.



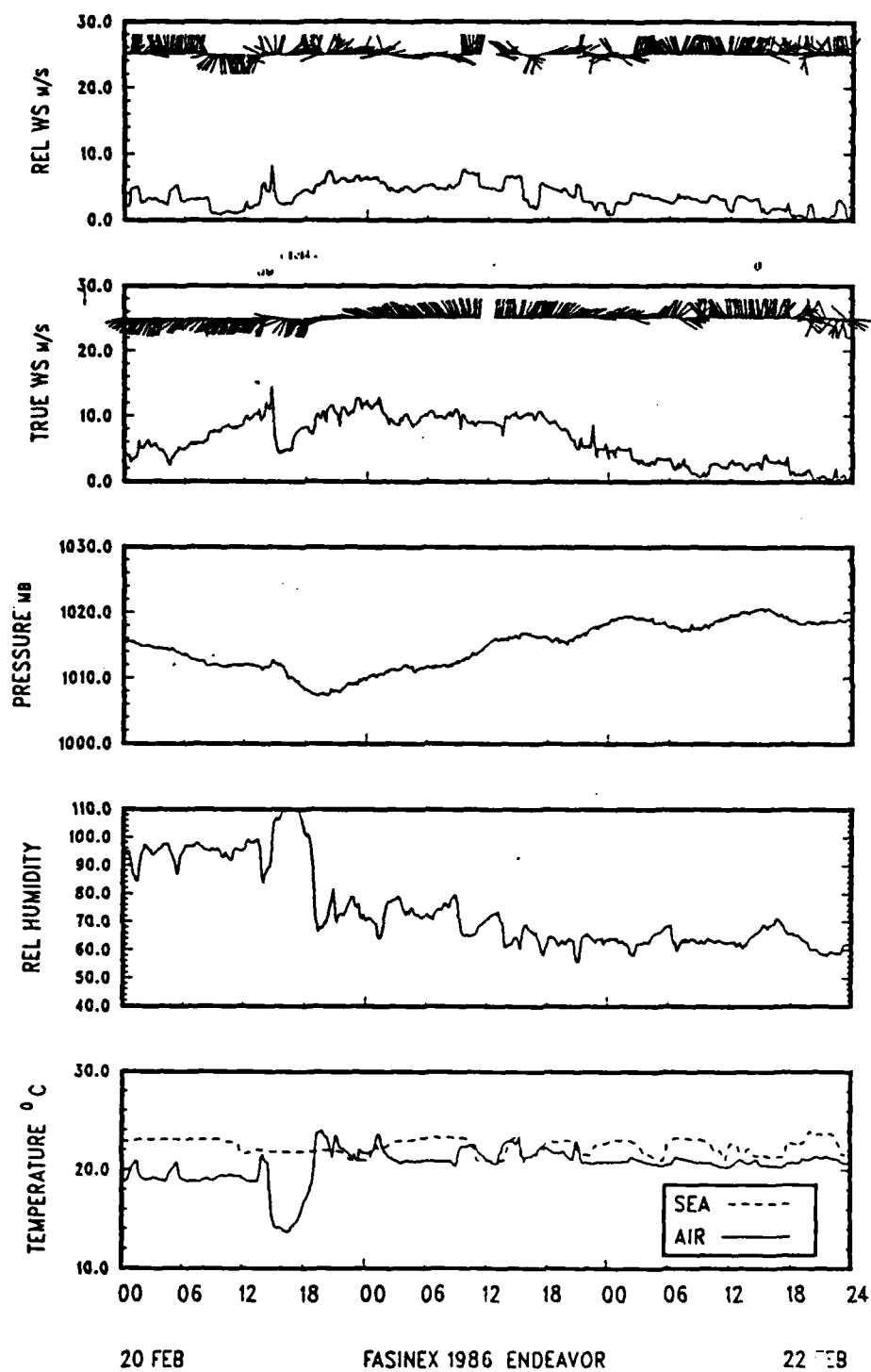


Figure 3.8 Time Series 20 Feb. - 22 Feb. 1986.

specific humidity decreasing with height below the inversion (Fig. 3.9).

The upper-level trough deepened and moved eastward out of the FASINEX area by 1200 GMT on 21 February (Fig. 3.7). Sea-level pressure increased to a maximum of 1019 mb as a weak sea-level high developed. Wind speed decreased to  $4 \text{ ms}^{-1}$  and wind direction shifted to the northeast. Unstable air-sea temperature differences of several degrees were present from 0000 to 1100 and 1900 to 0000 GMT (Fig. 3.8). There was a small amount of stratus present in a mostly clear sky. The mixed layer height was approximately 800 m (Fig. 3.9).

Synoptic-scale conditions were dominated by an upper-level ridge and the subtropical high on 22 February (Fig. 3.7). Sea-level pressure ranged from 1018-1020 mb. Wind speed dropped to  $1 \text{ ms}^{-1}$  by the end of the day and the wind direction shifted from northeast to southeast. Unstable air-sea temperature differences of 1-3°C degrees existed until the end of the period (Fig. 3.8). Small amounts of low-level stratus were present in an otherwise clear sky. The mixed layer height was about 1200 m (Fig. 3.9).

Evolution of the mixed layer was dominated in the beginning of the period by the approaching low pressure system. During the mid-period as a weak high pressure cell developed into a sea-level high pressure system the

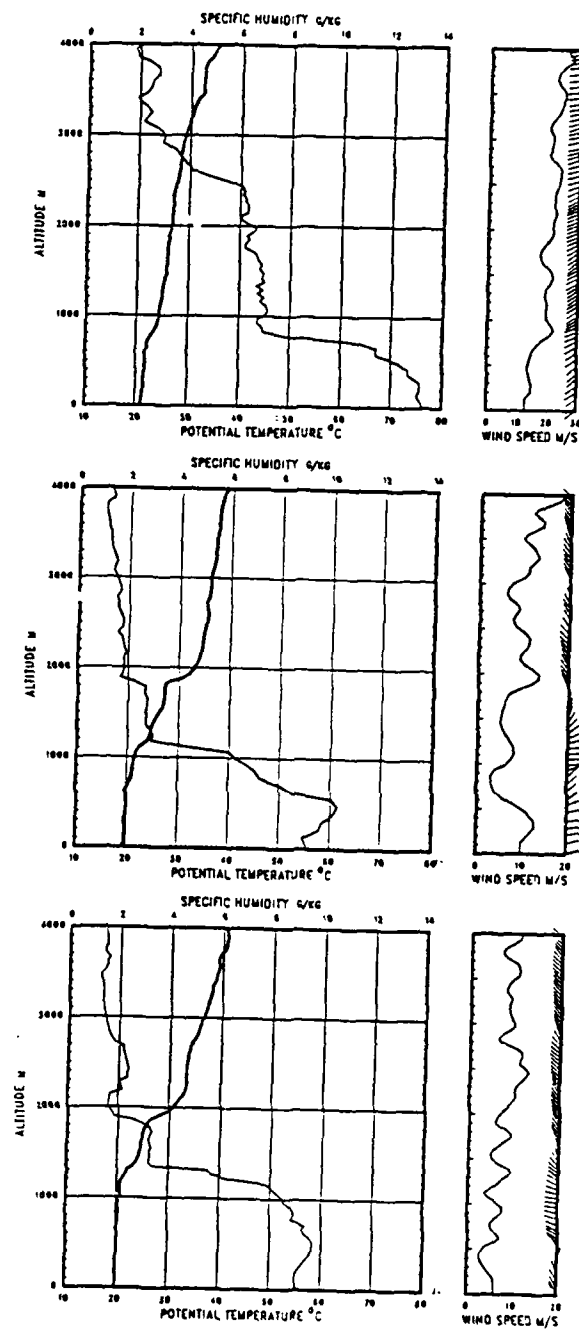


Figure 3.9 Radiosonde Profiles, 20 Feb. 86 (top),  
21 Feb. 86 (mid), 22 Feb. 86 (bot).

subsidence inversion became distinct at 2000 m and a lower convectively driven mixed layer extended up to 1200 m.

The synoptic-scale effects were dominant in the evolution of the mixed layer during this three day period. At the beginning, on the 20th, the near surface southwesterly flow maintained the distinct moist layer up to 800 m, with specific humidity above  $12 \text{ gkg}^{-1}$ , even with the approaching front. The absence of subsidence within the approaching front maintained the moisture at  $6 \text{ gkg}^{-1}$  up to 2500 m. With the passage of the trough and intensification of the subtropical high, the subsidence increased so that an inversion was evident at 2000 m on 22 February. The northwesterly flow with upwind cooler sea-level temperatures caused lower specific humidities in the mixed layer; near  $9 \text{ gkg}^{-1}$ . The increase of the mixed layer from 800-1200 m was presumably due to the increased convection associated with wind decreasing from  $12 \text{ ms}^{-1}$  on the 20th to  $6 \text{ ms}^{-1}$  on the 22nd.

#### 4. 23 February - 25 February 1986

The high pressure system continued to dominate the early part of this period. Synoptic-scale conditions changed gradually during the mid-period reflecting pre-frontal characteristics. At the end of the period an eastward moving cold front began to affect the synoptic-scale situation.

On 23 February, the upper-flow returned to a zonal pattern and the sea-level conditions were dominated by the subtropical high until 1200 GMT (Fig. 3.10). An advancing low pressure system caused the wind speed to increase to  $8 \text{ ms}^{-1}$  and the wind direction to shift to the southwest by 1800 GMT. The sea-level pressure ranged from 1016-1020 mb. An unstable air-sea temperature difference of  $2^{\circ}\text{C}$  existed until 1300 GMT when warm air advected over the cooler water causing conditions to stabilize until 0000 GMT (Fig. 3.11). Low-level stratus clouds were present with altostratus moving in at 1830 GMT. No precipitation was recorded. The mixed layer height increased from 1200 m early in the day to 2000 m by mid-day (Fig. 3.12).

The cold front stalled just west of the FASINEX area on 24 February causing the sea-level pressure to drop only slightly (Fig. 3.10). Wind speed ranged from  $5\text{-}8 \text{ ms}^{-1}$  and the direction was consistently from the southwest. An alternating stable/unstable air-sea temperature difference of  $1\text{-}2^{\circ}\text{C}$  existed throughout the period (Fig. 3.11). Cloud cover was composed of low-level stratus/stratocumulus with altostratus and cirrus appearing during the day. Rain was recorded at 1430 GMT, showers at 1713 GMT and heavy rain at 1900 GMT. The top of the mixed layer was approximately 2000 m. Potential temperature was well mixed below the inversion while specific humidity decreased with height (Fig. 3.12).

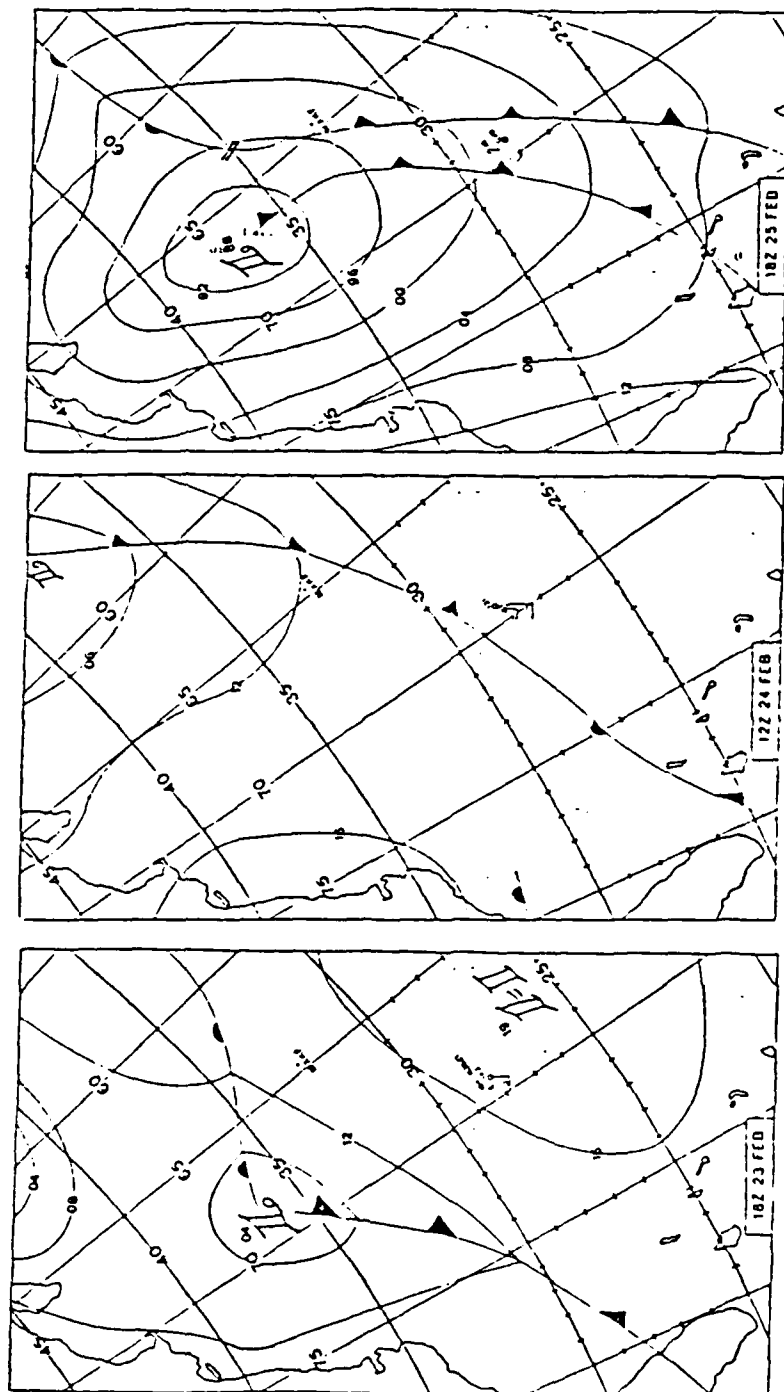


Figure 3.10 Surface Weather Map, 23 Feb. - 25 Feb. 1986.

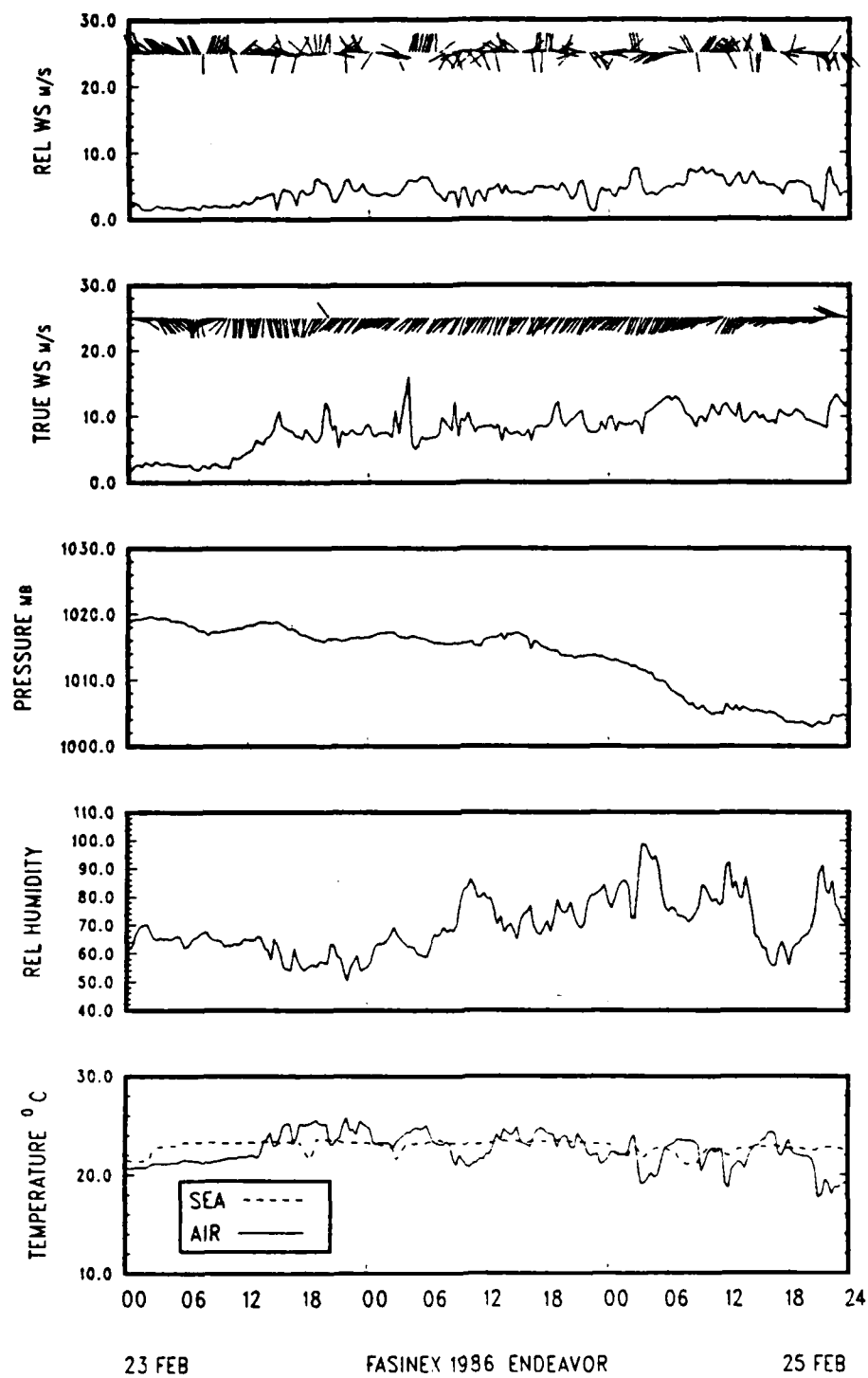


Figure 3.11 Time Series 23 Feb. - 25 Feb. 1986.

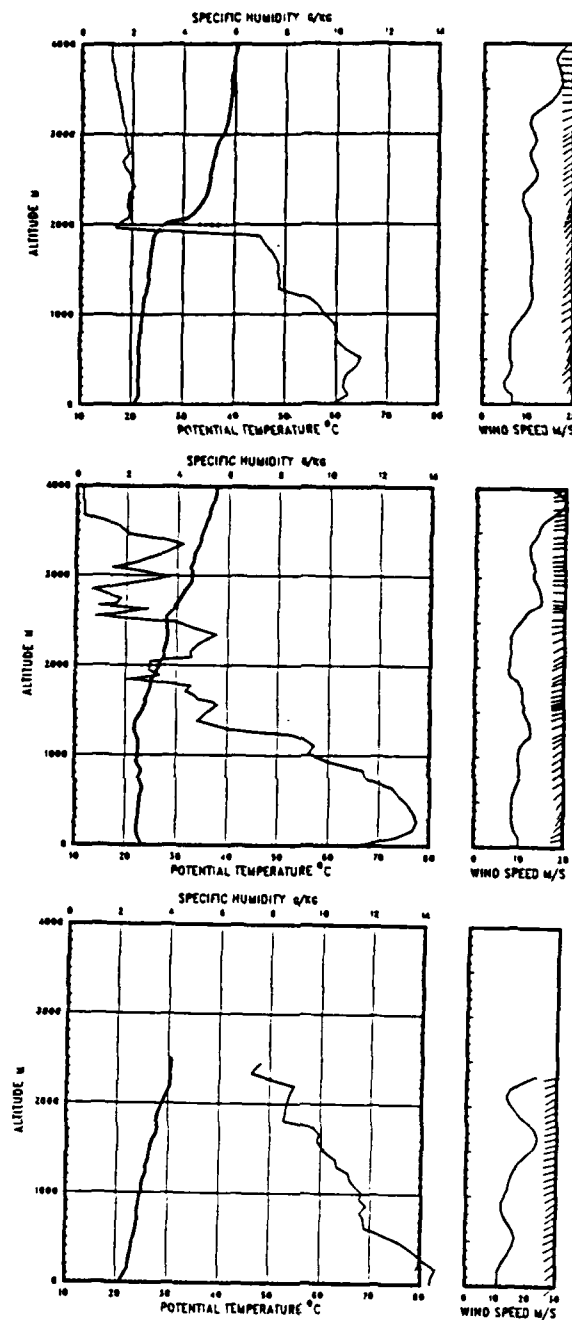


Figure 3.12 Radiosonde Profiles, 23 Feb. 86 (top),  
24 Feb. 86 (mid), 25 Feb. 86 (bot).



The cold front began moving eastward on 25 February causing the sea-level pressure to decrease steadily (Fig. 3.10). Wind speed increased to  $12 \text{ ms}^{-1}$  and the direction shifted to west-northwest. The cold front developed rapidly (and passed through the FASINEX area at 2000 GMT) causing the sea-level pressure to drop to 1003 mb. Alternating stable/unstable air-sea temperature differences of several degrees persisted throughout the day (Fig. 3.11). Mid-level altostratus and cirrus clouds were present in the early part of the day and gave way to partial clearing by 1300 GMT. At 2000 GMT, low to mid-level stratus/stratocumulus clouds moved in. Rain occurred from 1000 to 2130 GMT with heavy rain noted at 2030 GMT. The mixed layer was slightly evident during this period (Fig. 3.12).

There is minimal change in the mixed layer depth during this period in the weakening high, with an approximate height of 2000 m.

This period illustrates the typical mixed layer changes which would occur in a passage of a weak frontal system in the subtropical region. On the 23rd, the cloud top mixed layer is well defined extending up to 1900-2000 m. Evidence of saturation (cloud) is distinct from 1100 m to 1900 m with the decrease in specific humidity. A distinct near-surface stable layer, extending to 150 m is evident in the vector wind profile as well as in the temperature and specific humidity profiles. The wind direction changes from

southeast to southwest at the top of this layer. The change in wind speed (from 6-12  $\text{ms}^{-1}$ ) and wind direction (from 200°-250°) at cloud base is interesting but unexplained.

On the 24th, the approach of the trough is apparent with the moist layer, above 4  $\text{gkg}^{-1}$ , extending up to 2500 m. The OCEANUS sounding shows a specific humidity of 8  $\text{gkg}^{-1}$  extending up to 2200 m at 0600 GMT. The sea-level upwind layer decreased to 1200 m with an unstable layer at 1250 m. The profile for this period is considered as being a transition with synoptic-scale evolutions. The absence of elevated layers in the 1200 GMT profile of the 25th reflects the influence of the trough passing the FASINEX area around 1800 GMT.

#### 5. 26 February - 28 February 1986

The low pressure system centered north of the FASINEX area continued to dominate the synoptic-scale conditions throughout this period. Additionally, a secondary low pressure system off the US east coast began to influence the synoptic-scale conditions by the 27th.

Although the center of the low pressure system of the previous day remained well to the north, it dominated the synoptic-scale situation on 26 February (Fig. 3.13). The system's central pressure dropped to 982 mb, while the upper-level trough developed into a closed low. This produced a strong sea-level gradient and maximum wind speeds

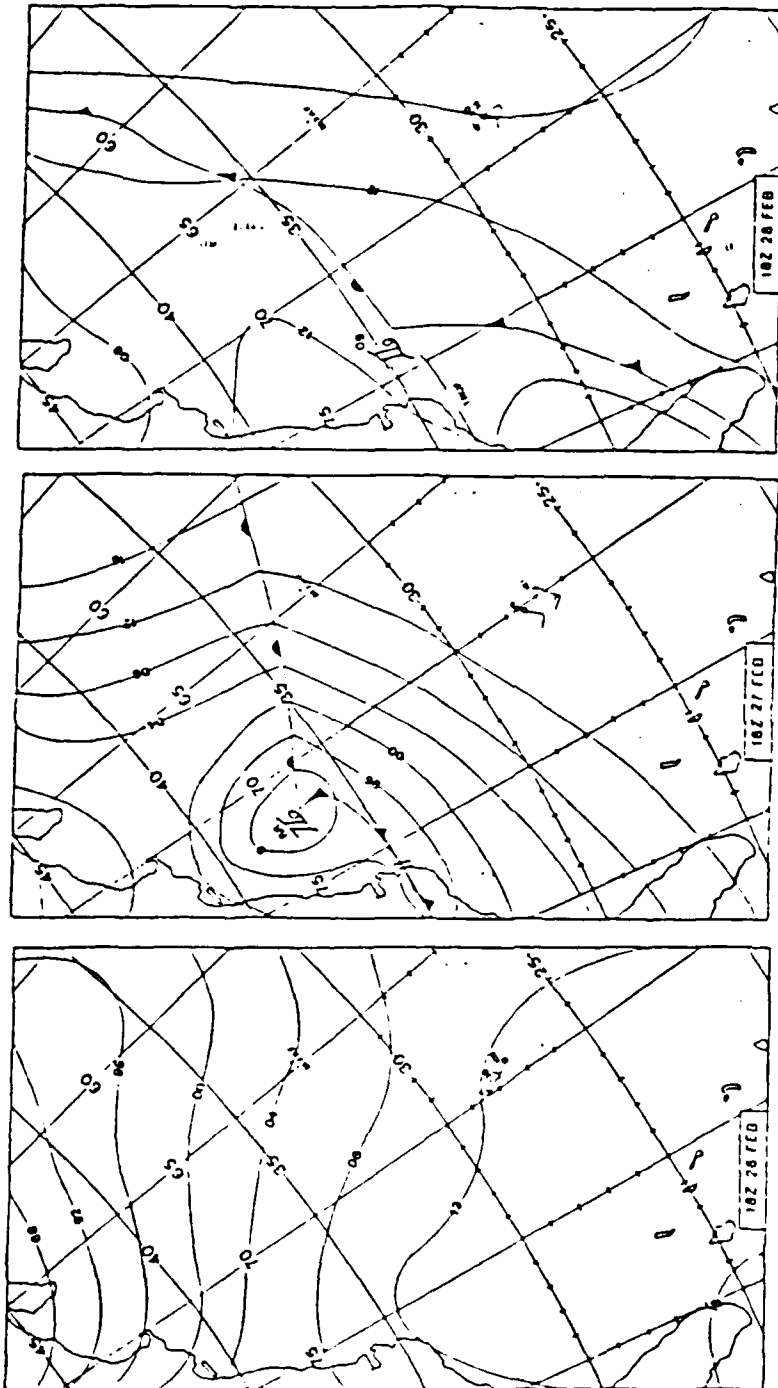


Figure 3.13 Surface Weather Map, 26 Feb. - 28 Feb. 1986.

of  $15 \text{ ms}^{-1}$  in the FASINEX area (0800-1400 GMT). The constant northwest wind direction produced a sea swell of 4-5 m, which decreased to 1-2 m. Sea-level pressure rose to 1016 mb and wind speed dropped to  $3 \text{ ms}^{-1}$  by 0000 GMT as a weak high pressure cell began to develop. Unstable air-sea temperature differences of  $2-6^{\circ}\text{C}$  were present during the beginning of the period (Fig. 3.14). Cloud cover consisted of low to mid-level stratus/stratocumulus with the mid-level altostratus appearing by 1800 GMT. Clearing occurred at 1900 GMT. Heavy rains were recorded at 0600 GMT. The mixed layer height was 1500 m (Fig. 3.15).

Synoptic-scale conditions were influenced by a low pressure system just off the US east coast on 27 February. This system moved in a north-northeast direction due to an upper-level trough over the eastern United States (Fig. 3.13). Sea-level pressures were steady, ranging from 1016-1018 mb. The wind shifted to southwest and decreased to  $2 \text{ ms}^{-1}$  at 0200 GMT. Unstable air-sea temperature differences of  $2-6^{\circ}\text{C}$  persisted (Fig. 3.14). Low to mid-level stratus clouds cleared by 1830 GMT. No precipitation was noted. The mixed layer height lowered to 1600 m by mid-period, suggesting subsidence was occurring (Fig. 3.15).

The low pressure system continued to dominate the synoptic-scale situation on 28 February (Fig. 3.13). Sea-level pressure remained steady at 1016-1018 mb and the wind was from the southwest at  $6-10 \text{ ms}^{-1}$ . Unstable air-sea

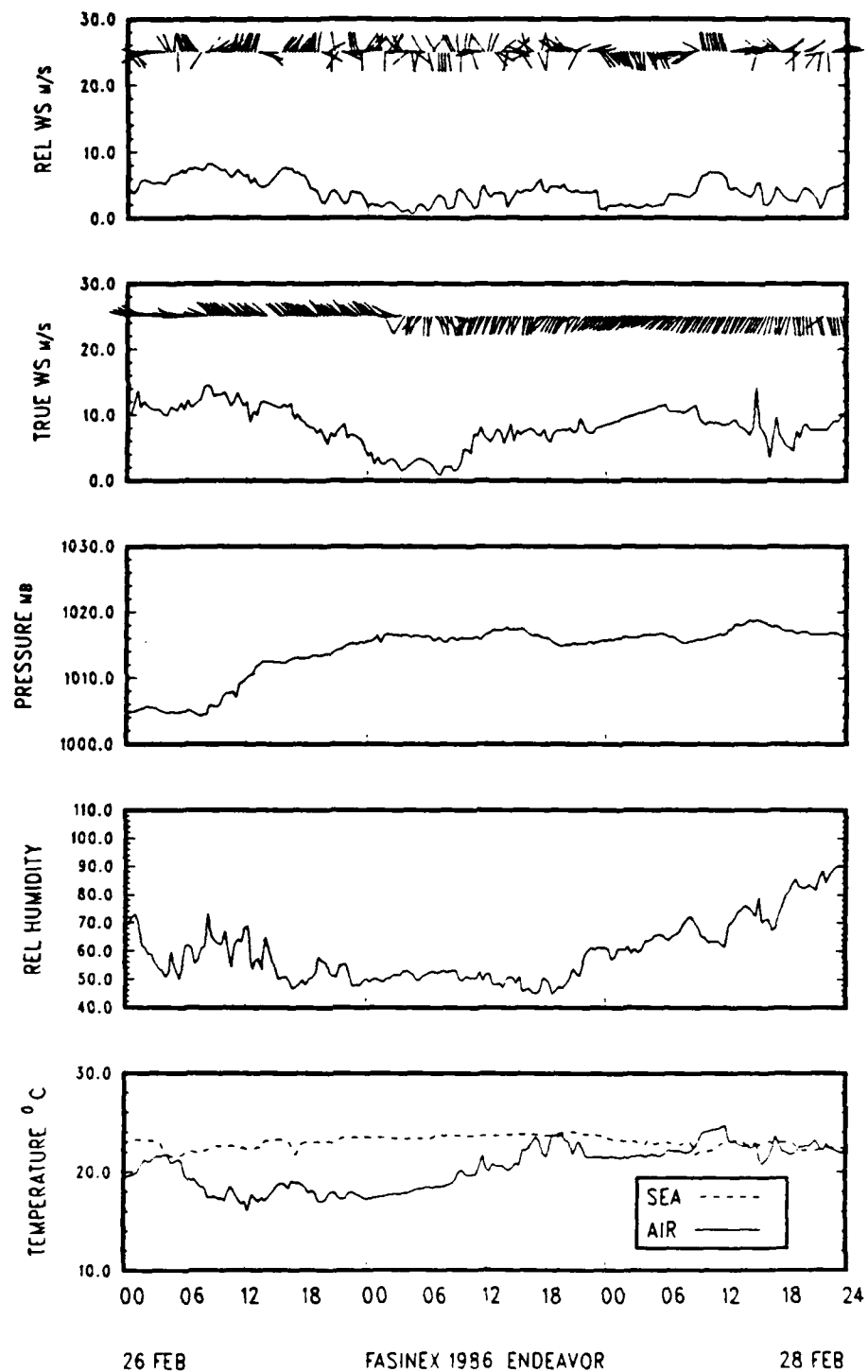


Figure 3.14 Time Series 26 Feb. - 28 Feb. 1986.

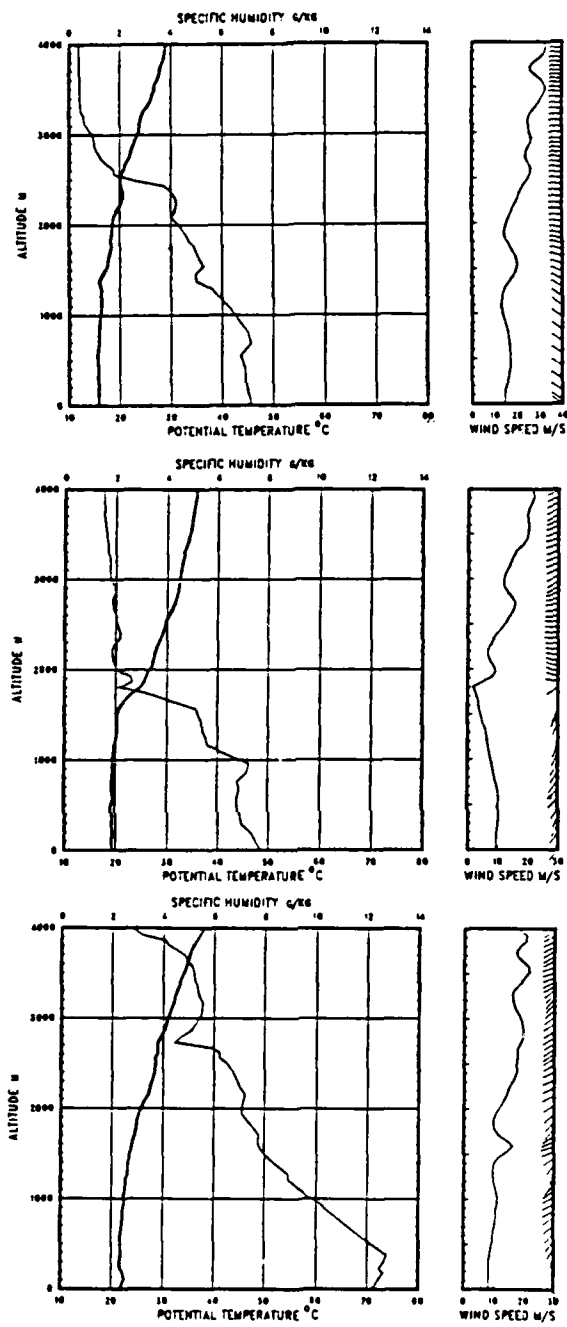


Figure 3.15 Radiosonde Profiles, 26 Feb. 86 (top),  
27 Feb. 86 (mid), 28 Feb. 86 (bot).

temperature differences of  $2^{\circ}\text{C}$  continued to exist until 0400 GMT when warmer air was advected over the cooler water, stabilizing conditions. At 1400 GMT conditions returned to unstable and remained that way until 1600 GMT and again stabilized until 0000 GMT (Fig. 3.14). Some low-level stratus clouds were present and a heavy rainshower occurred at 1700 GMT. A mixed layer is not clearly evident in Fig. 3.15.

The evolution of the vertical profiles during this period was influenced by both the upper-level convergence, associated with the wave formation off the east coast, and the near-surface flow.

On the 26th, the weak influence of the subtropical high caused the subsidence inversion to occur near 2500 m. The northwesterly flow, over cooler waters, caused the mixed layer temperature to be less than  $17^{\circ}\text{C}$  and the specific humidity to be less than  $7\text{ gkg}^{-1}$ . The profiles exhibit features associated with subtropical shallow convection.

On the 27th, with southwesterly flow, the mixed layer depth appears to decrease. The wind direction is northwest to west up to 4000 m. This inversion is due to a change in air masses when wind direction changes from south southwest to west at the height of the inversion. The air mass change is pronounced in the mixed layer temperature which increases from  $16^{\circ}\text{C}$  to above  $19^{\circ}\text{C}$  and increases in both the temperature and humidity above the inversion.

On the 28th, the flow in the lower-layer becomes true southerly and causes increases in both the mixed layer temperature (from 19°-22° C) and specific humidity (from 8-13 gkg<sup>-1</sup>). The layer above the immediate sea-level influence, above 1000 m, shows the effect of the approaching trough with transistional features.

6. 01 March - 03 March 1986

The beginning part of this period had synoptic-scale characteristics typical of a pre-frontal situation. A cold front passed through the FASINEX area during mid-period, while the end of the period saw the development of a sea-level high pressure system centered to the southwest (Fig. 3.16).

On 1 March an advancing low pressure system caused the sea-level pressure to drop from 1017-1010 mb in 18 hours (Fig. 3.17). Wind direction was southerly with speed increasing from 10 to 18 ms<sup>-1</sup>. An air-sea temperature difference of 1-2°C was present until 1700 GMT when a cold air mass increased the difference to 4-12°C until 0000 GMT (Fig. 3.17). Cloud cover consisted of mid-level altostratus/altocumulus with some cirrus occurrence by 1030 GMT. Heavy rain was noted at 1900 GMT. The mixed layer depth is poorly defined (Fig. 3.18).

The cold front passed through the FASINEX area at 0000 GMT on 2 March (Fig. 3.16). Sea-level pressure rose steadily to 1018 mb during the day. Windspeed dropped from



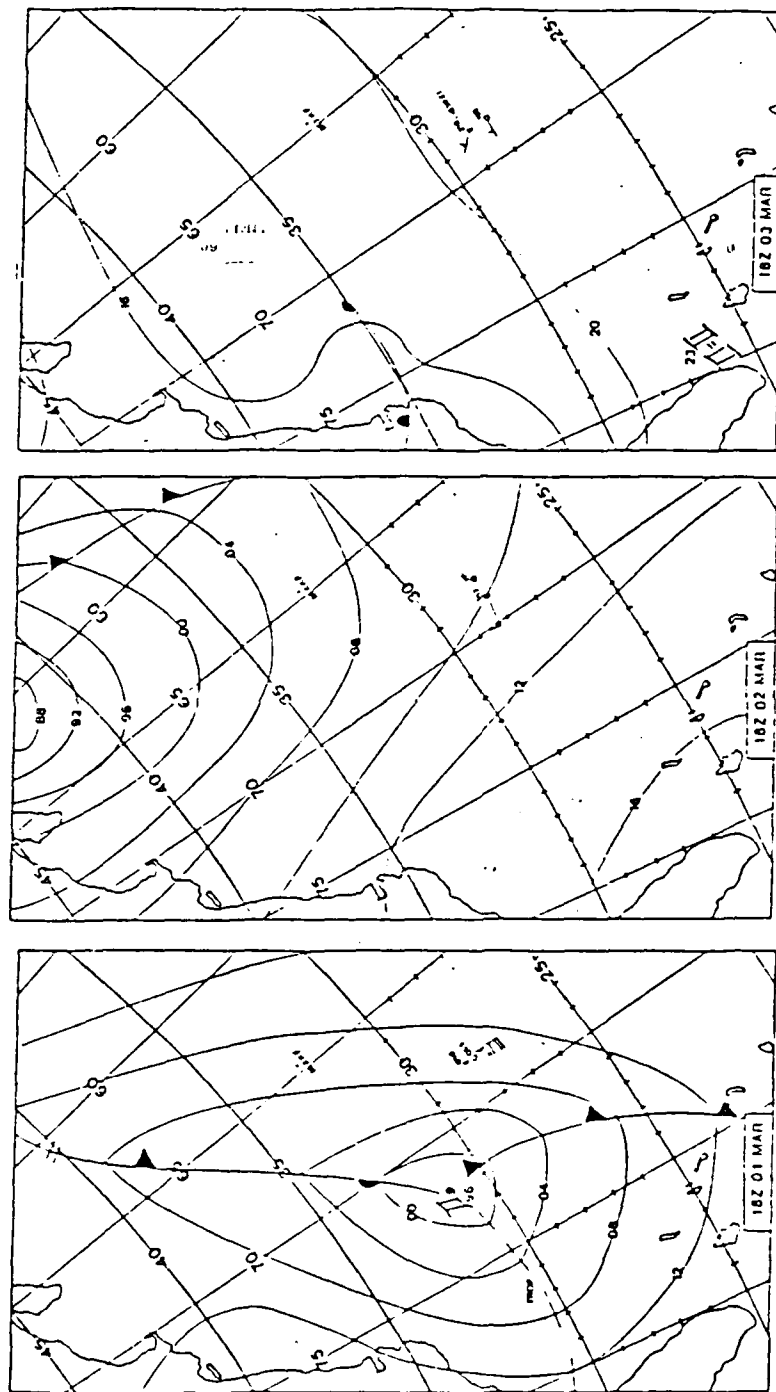


Figure 3.16 Surface Weather Map, 01 Mar. - 03 Mar. 1986.

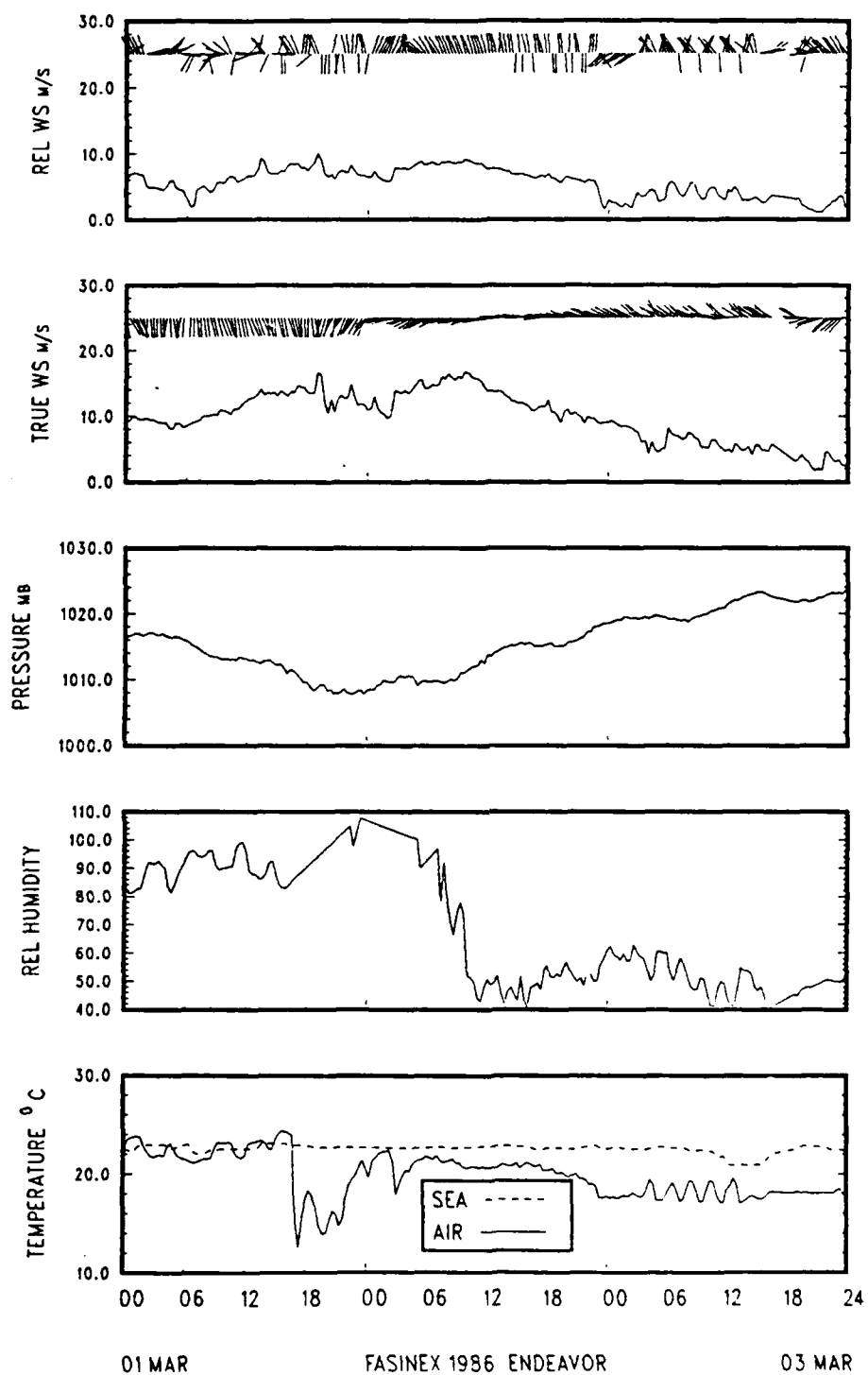


Figure 3.17 Time Series 01 Mar. - 03 Mar. 1986.

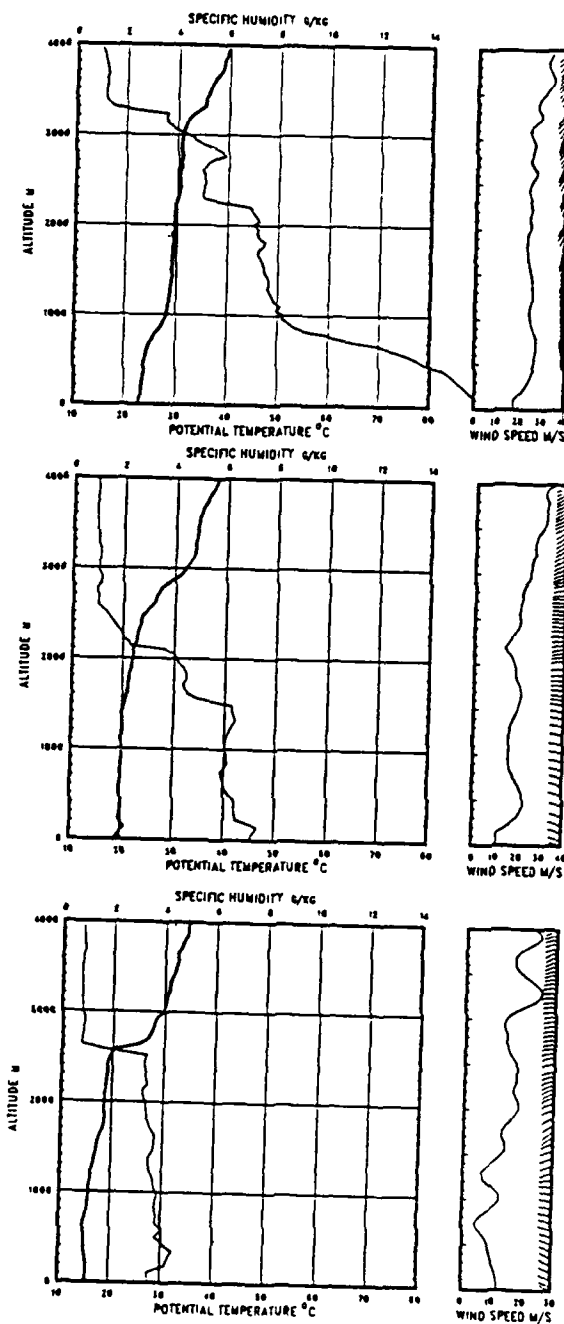


Figure 3.18 Radiosonde Profiles, 01 Mar. 86 (top),  
02 Mar. 86 (mid), 03 Mar. 86 (bot).

16-10  $\text{ms}^{-1}$  and wind direction shifted to west-southwest after the frontal passage. An unstable air-sea temperature difference of 1-4°C existed until 0000 GMT on 3 March (Fig. 3.17). Relative humidity decreased from 100%-42% in 6 hours (0600-1200 GMT) and remained quite low until the end of the period. Stratus and altostratus clouds were present and no precipitation was noted. The mixed layer is again poorly defined (Fig. 3.18).

On 3 March the upper-level trough began deepening as a sea-level high developed to the southwest (Fig. 3.16). Sea-level pressure increased from 1018-1023 mb in 24 hours. Wind speed decreased steadily from 10-3  $\text{ms}^{-1}$ . Wind direction was from the northwest until 1800 GMT when it shifted to the southwest due to an advancing cold front. The unstable air-sea temperature difference of 2-4°C persisted until the end of the period (Fig. 3.17). Low and mid-level stratus/stratocumulus were present. The mixed layer height is approximately 2600 m (Fig. 3.18).

Changes in vertical profiles of temperature and humidity over these three days clearly show the effect of differential advection in forming layers. The effects are most pronounced in the specific humidity profiles. Minimal effects on the local sea-level temperature fields would be expected on these days.

On 1 March when the FASINEX area was in the warm sector of a rapidly approaching frontal system, the lower-

layer had southerly flow and was characterized by being very moist with specific humidity above  $15 \text{ gkg}^{-1}$  up to 300 m. Above 1000 m the wind direction shifted to southwest and the specific humidity decreased to below  $8 \text{ gkg}^{-1}$ . Above 2200 m, the wind direction shifted more to the west and the specific humidity dropped below  $6 \text{ gkg}^{-1}$ .

On 2 and 3 March, the profiles reflected changes associated with locations in the cooler and drier air behind the rapidly moving frontal system. The subsidence inversion on both days was above 2200 m. From 2-3 March the mixed layer temperature decreased from  $20^{\circ}$ - $15^{\circ}\text{C}$ , and specific humidity from  $6$ - $4 \text{ gkg}^{-1}$ .

#### 7. 04 March - 06 March 1986

Pre-frontal conditions existed during the start of this period associated with a rapidly developing sea-level low pressure system. This system was steered into the FASINEX area by an upper-level trough. This low pressure system dominated until a weak high pressure cell developed late in the period.

Sea-level conditions were influenced by the warm sector of the frontal system which stalled west of the FASINEX area on 4 March (Fig. 3.19). Sea-level pressure ranged from 1020-1023 mb. Wind was from the southwest at  $2$ - $6 \text{ ms}^{-1}$ . Unstable air-sea temperature differences of  $1$ - $2^{\circ}\text{C}$  were present until 0000 GMT (Fig. 3.20). Cloud cover

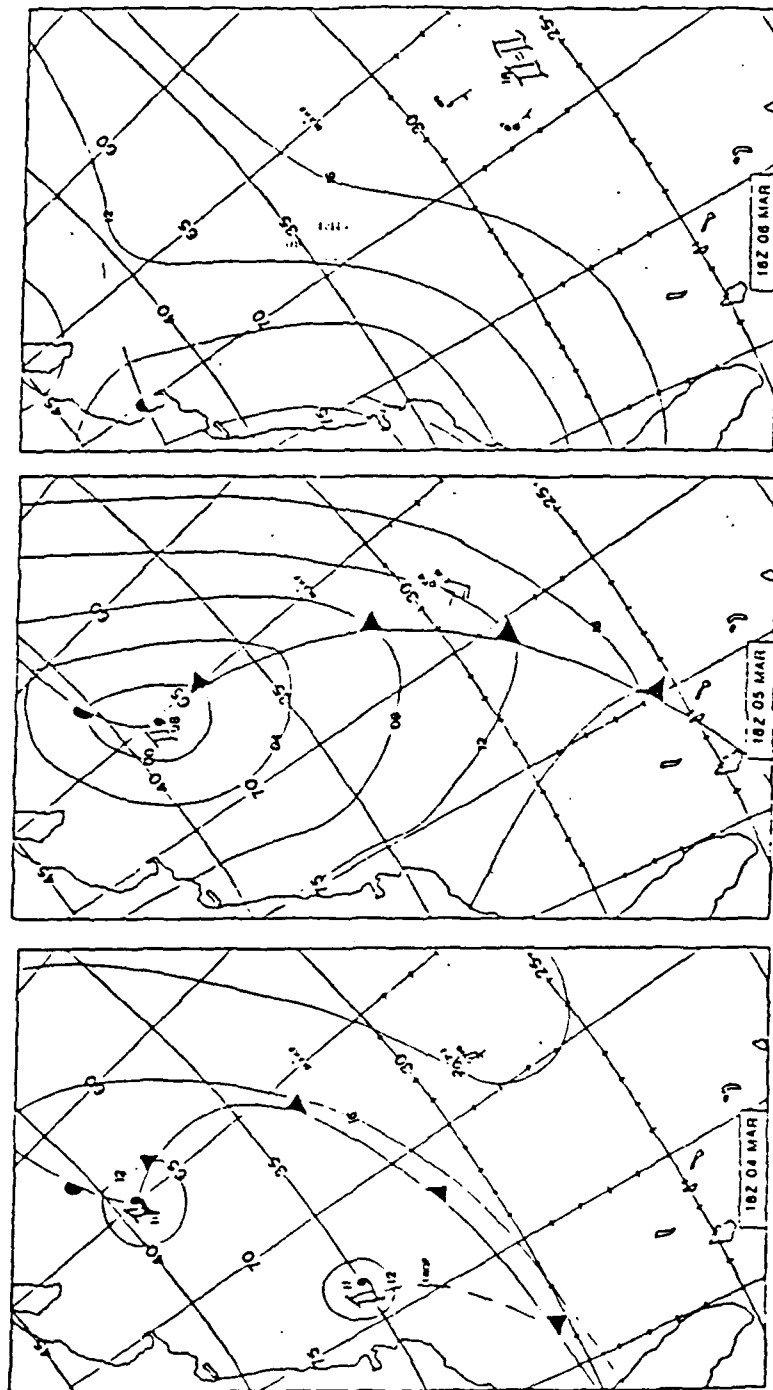


Figure 3.19 Surface Weather Map, 04 Mar. - 06 Mar. 1986.

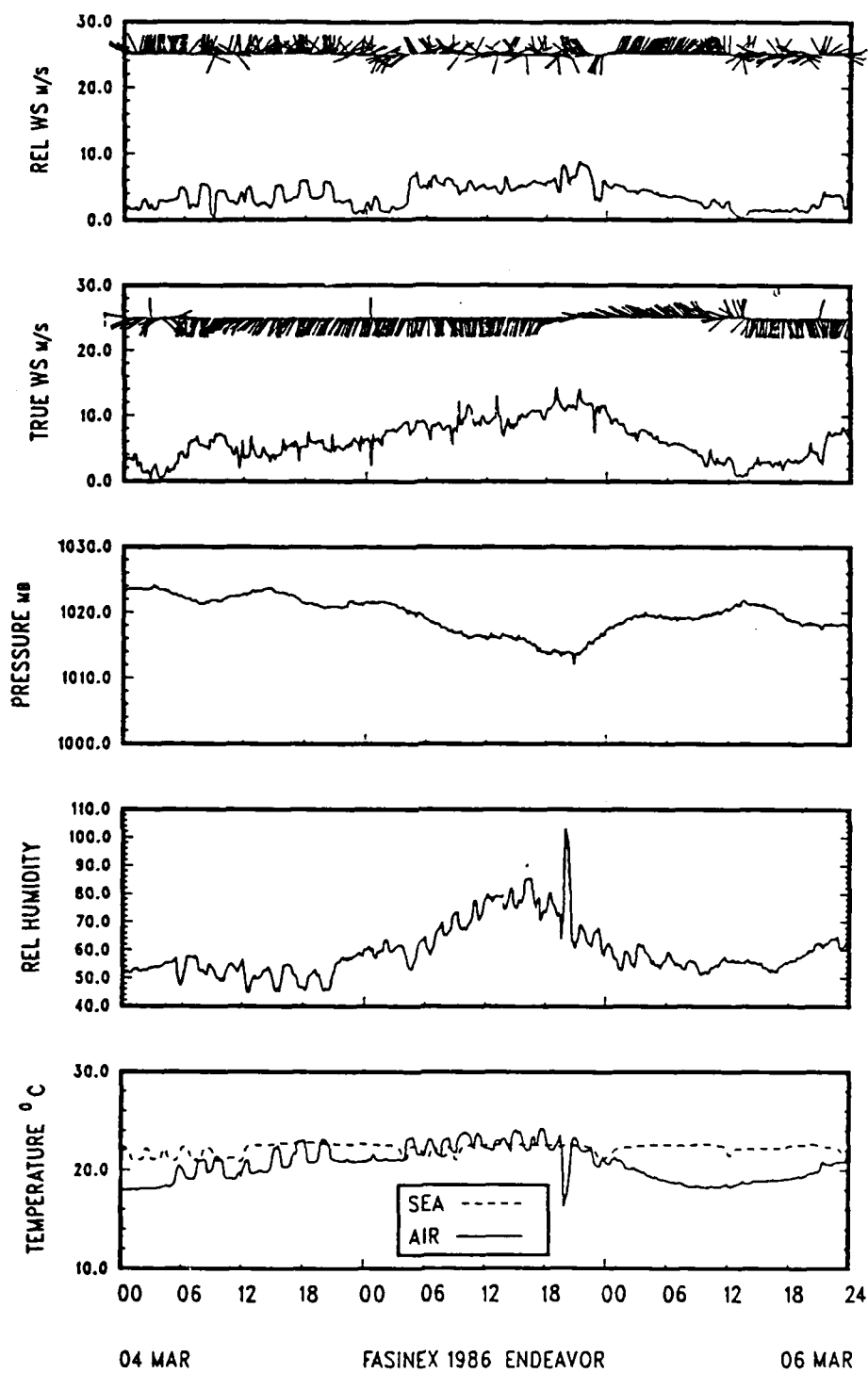


Figure 3.20 Time Series 04 Mar. - 06 Mar. 1986.

consisted of mostly low to mid-level stratus with small amounts of cirrus appearing at 1830 GMT. No precipitation occurred. The mixed layer height is 1800 m with potential temperature well mixed and specific humidity decreasing with height below the inversion (Fig. 3.21).

The deepening upper-level trough over the eastern United States steered the sea-level low pressure system on a northeastward track bringing the cold front into the FASINEX area on 5 March (Fig. 3.19). Sea-level pressure dropped to a minimum of 1012 mb and wind speed reached a maximum of  $14 \text{ ms}^{-1}$  during the frontal passage (1900 GMT). The wind direction shifted from southwest to northwest. Air-sea temperature differences of  $1\text{--}2^{\circ}\text{C}$  fluctuated between stable and unstable conditions until 0000 GMT (Fig. 3.20). Mid to upper-level altostratus/cirrus clouds gave way to partial clearing and low-level stratus by 2000 GMT. Light rain was noted at 0100 and 0800 GMT. The mixed layer height is 2300 m with potential temperature well mixed and specific humidity decreasing with height (Fig. 3.21).

The upper-level trough and sea-level frontal system had passed through the region by 1200 GMT on 6 March (Fig. 3.19). Sea-level pressure rose to 1022 mb, wind speed decreased to  $1 \text{ ms}^{-1}$  and wind direction shifted to the southwest as a weak high pressure cell developed. An unstable air-sea temperature difference of  $2\text{--}4^{\circ}\text{C}$  lasted until the end of the period (Fig. 3.20). Mostly low to



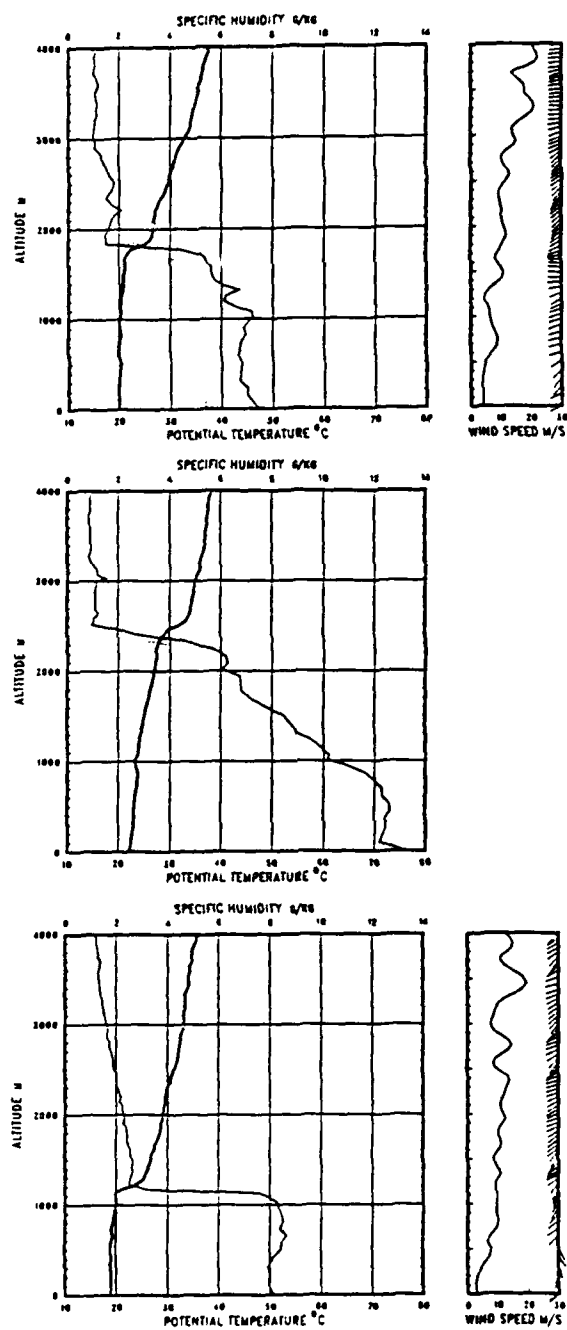


Figure 3.21 Radiosonde Profiles, 04 Mar. 86 (top),  
05 Mar. 86 (mid), 06 Mar. 86 (bot).

mid-level stratus clouds were present and no precipitation was recorded. The mixed layer height is 1200 m with potential temperature and specific humidity well mixed below the inversion (Fig.3.21).

During these three days the profiles exhibited the differences between an air mass moving out of the area, a frontal system in the area and the intensification of the subtropical high.

On the 3rd, the mixed layer had decreased to below 2000 m, from 2600 m on the 3rd, due to subsidence in the tracking path part of the transiting high. This increase of potential temperature at 4000 m from  $38^{\circ}$ - $39^{\circ}$ C between 1500 GMT on the 3rd to 1300 GMT on the 4th is evidence of the occurrence of subsidence. The mixed layer temperature had increased from  $15^{\circ}$ - $20^{\circ}$ C and specific humidity from  $3.5$ - $7 \text{ gkg}^{-1}$  respectively due to flow being southerly on the 4th versus northwesterly on 3 March. This illustrates the effect of upwind sea-level temperatures.

On the 5th, the approaching front and convergence zone caused a decrease in the subsidence and the inversion increased due to convection and, perhaps, upwind mean velocity to 2500 m. The mixed layer adjacent to the sea-level had increased in temperature (from  $20^{\circ}$ - $22^{\circ}$ C) and specific humidity (from  $7$ - $12 \text{ gkg}^{-1}$ ) due to increasing winds and, hence, advection from warmer water regions. On the 6th, re-establishment of the subtropical high over the

FASINEX area with light winds caused a well defined convection mixed layer with slightly lower temperature and significantly lower specific humidity (from 12-8 gkg<sup>-1</sup>). The reduction in specific humidity is believed to be associated with increased entrainment of overlying icy air during this convectively driven low wind period.

Both the 4 March and 6 March mixed layer features were expected to have been influenced by sea-level as well as synoptic-scale forcing.

#### 8. 07 March - 09 March 1986

A weak high pressure cell was being replaced by a developing sea-level low pressure system at the beginning of this period. The low pressure system dominated the FASINEX area synoptic-scale situation for approximately 24 hours when upper-level flow returned to normal and a high pressure system intensified behind the front.

On 7 March an upper-level trough and a sea-level low pressure system developed over the northeastern United States (Fig. 3.22). This system had little influence in the FASINEX area other than to shift the wind direction to the southwest. Sea-level pressure ranged from 1014-1016 mb. Wind speed ranged from 4-10 ms<sup>-1</sup>. An unstable air-sea temperature difference of 2-4°C dominated the entire period (Fig. 3.23). Fig. 3.23 is based on OCEANUS data because data from ENDEAVOR are unavailable after 7 March. The absence of ENDEAVOR data means most vector wind profiles

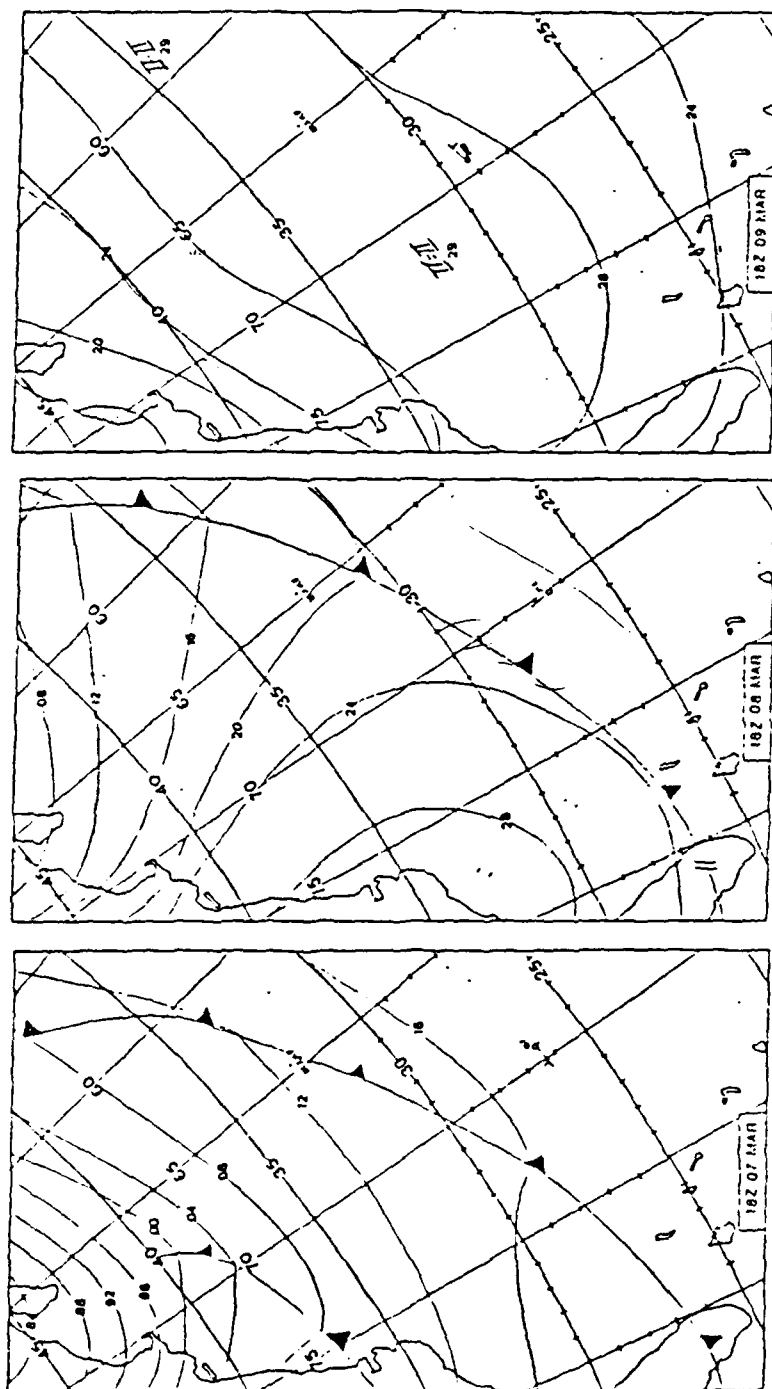


Figure 3.22 Surface Weather Map, 07 Mar. - 09 Mar. 1986.

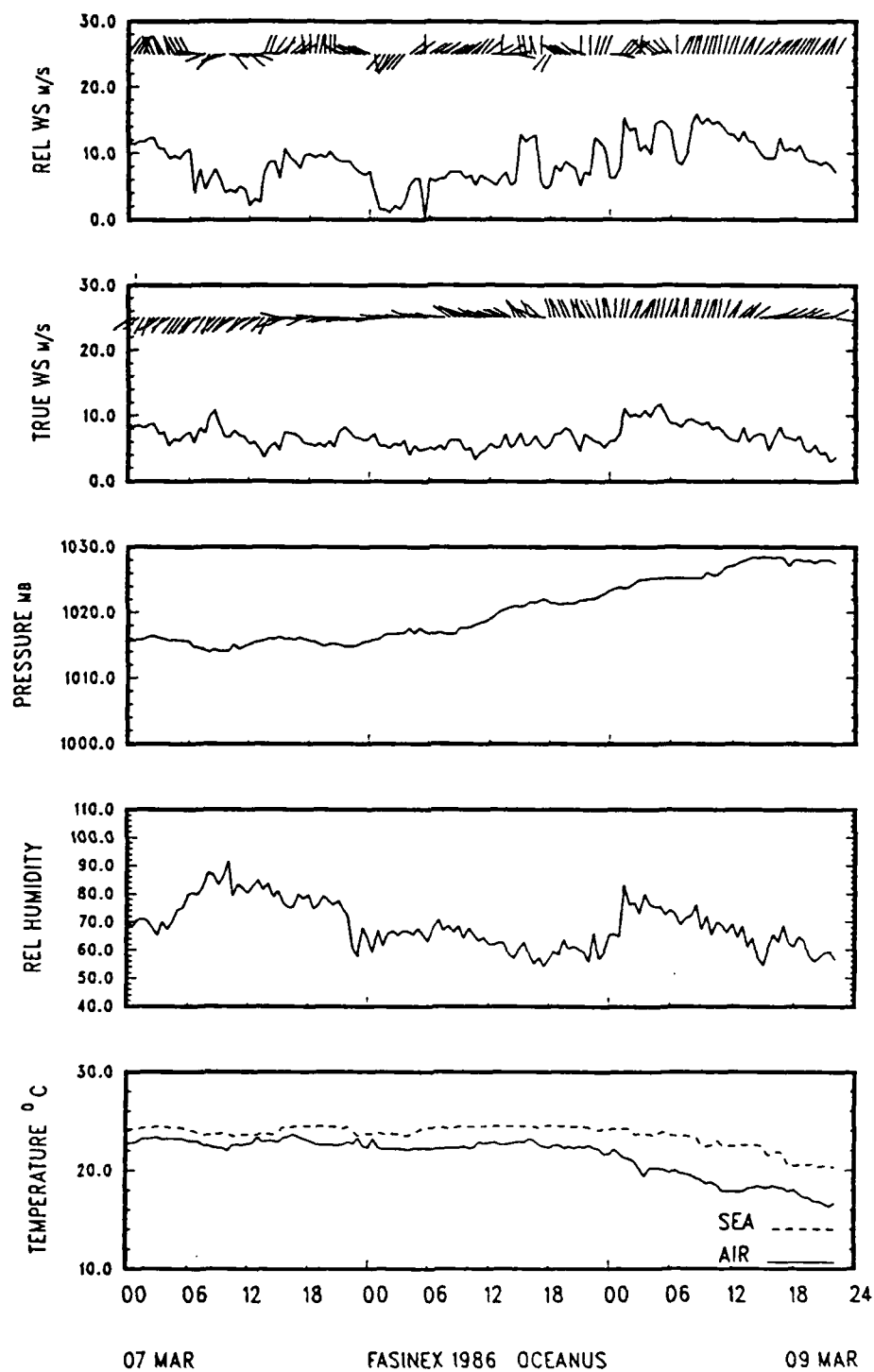


Figure 3.23 Time Series 07 Mar. - 09 Mar. 1986.

will not be shown. The skies were mostly clear although rain showers occurred at 1430 GMT. The mixed layer depth is 800 m with potential temperature and specific humidity well mixed below the inversion (OCEANUS Fig. 3.24).

Synoptic-scale conditions were dominated by high pressure and the passage of a frontal remnant associated with the low pressure system of the previous day on 8 March (Fig. 3.22). A frontal passage occurred at 0800 GMT and only caused a slight shift in the wind direction from west to northwest. Sea-level pressure rose steadily from 1014-1022 mb (Fig. 3.23, OCEANUS). Some low-level stratus clouds were present, but no precipitation was recorded. Mixed layer height increased from 800-1800 m by 1800 GMT. Potential temperature and specific humidity were well mixed below the inversion (Fig. 3.24, OCEANUS).

The upper-level flow returned to a zonal pattern and the sea-level conditions were dominated by the high pressure system on 9 March (Fig. 3.22). Sea-level pressure increased steadily to 1028 mb by 0000 GMT on 10 March. Wind speed decreased steadily from a high of  $10 \text{ ms}^{-1}$  to a low value of  $2 \text{ ms}^{-1}$  throughout the day (Fig. 3.23). Cloud cover consisted of mid-level altostratus with small amounts of cirrus. The mixed layer height is 1500 m with potential temperature and specific humidity well mixed below the inversion (Fig. 3.24, OCEANUS).

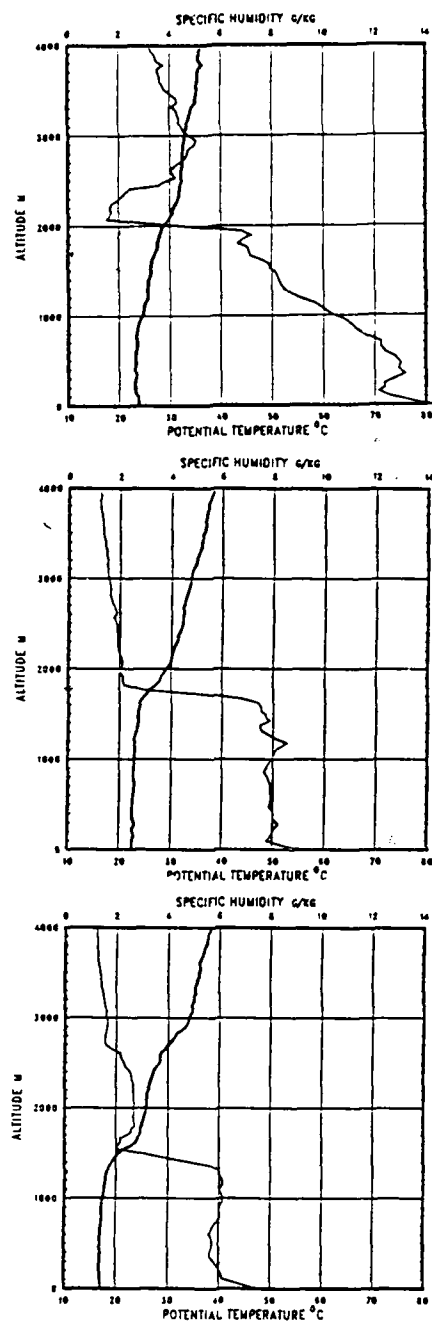


Figure 3.24 Radiosonde Profiles, 07 Mar. 86 (top),  
08 Mar. 86 (mid), 09 Mar. 86 (bot).

The weak high pressure cell continued to decrease the mixed layer depth to 800 m. As a sea-level low pressure system developed the inversion height increased to 1000 m due to mixing. At the end of the period evolution of the mixed layer depth was again controlled by a high pressure system which decreased the inversion to 1500 m.

The profiles on these days appear to show the effects of the synoptic-scale condition as well as the location of the OCEANUS being well south of the ocean front on the first two days (7th and 8th) and north of the front on the last (9th). The difference between the profiles of mixed layer specific humidity on the 7th and 8th is of interest because their locations had clear skies with regard to NMC position of the approaching front. Actually the front, based on pressure rise and wind shift, passes the R/V OCEANUS location about 0800 on the 8 March.

The difference due to frontal passage is illustrated by the specific humidity below 800 m. On 7 March it is above  $12 \text{ gkg}^{-1}$  while on 8 March it is  $8 \text{ gkg}^{-1}$ . It is expected that the deep convection with rain showers on the 7th affected the specific humidity throughout this layer. This could have been a local condition at the launch time. The profiles exhibit the convectively driven well-mixed features.



The profile evolution from the 8th to the 9th is due to location changes with respect to the post frontal high and the sea-level front.

From the 8th to the 9th the well mixed temperature has decreased from 22-17°C and the specific humidity has decreased from 8-6 gkg<sup>-1</sup>. The mixed layer depth, decreasing from 1800 to 1400 m, could be associated with increased subsidence and decreased convective driven entrainment. It is noted that the sea-level unstable air-surface temperature difference measured from 2°C on the 8th to 4°C on the 9th. Hence, entrainment with 5-8 ms<sup>-1</sup> winds should have been greater on the 9th.

This case clearly illustrates the response of mixed layer stratus to local as well as upwind sea-level temperature.

#### B. PROFILE PROPERTIES

Thirteen FASINEX rawinsonde sounding pairs were examined for the effect of sea surface temperature (SST) effects on the MABL. A sounding pair consists of one launch from OCEANUS and one launch from ENDEAVOR. These pairs were chosen by time of launch (within 60 minutes of each other) and relative proximity to the oceanic front (warm side/cold side). For seven pairs, soundings were taken on opposite sides of the oceanic front. For five pairs both soundings were taken on the warm side of the front and for one pair

soundings were taken on the cold side of the front (see Table III).

The oceanic front was determined by using the  $21^{\circ}\text{C}$  sea-surface temperature as the dividing value since the sea temperature across the front ranged from  $20\text{--}22^{\circ}\text{C}$ . All SST values less than  $21^{\circ}\text{C}$  were considered as cold side locations while all SST values greater than  $21^{\circ}\text{C}$  were considered as warm side locations.

The first two pairs were on 17 and 18 February when a subtropical high pressure system was in the FASINEX area. Sea-level pressure was decreasing and wind speed was  $6\text{--}8\text{ ms}^{-1}$  from the southeast. The first pair of soundings, made on 17 February at 2352 GMT and 18 February at 0049 GMT, were from opposite sides of the oceanic front, ENDEAVOR on the cold side and OCEANUS on the warm side. The distance between the ships was 44 km. Wind direction across the front is from the warm side to the cold side. The two profiles (Fig. 3.25) show potential temperature and specific humidity from each side of the front to be fairly similar. The mixed layer height on the warm side is approximately 200 m higher and more moist than on the cold side. The warm side sounding shows a stable condition for the first 300 m then becoming well mixed. The sounding from the warm side has layers of higher moisture between 0-300 m, 1000-1300 m, and 1300-4000 m. The cold side specific humidity is higher at 300-1000 m and at 1300-1700 m.

TABLE III

## RAWINSONDE PAIRS

SHIP	DATE	TIME	RELATION TO FRONT	SHIP SEPARATION DISTANCE
ENDEAVOR	17 FEB	2352Z	COLD SIDE	44 KM
OCEANUS	18 FEB	0049Z	WARM SIDE	
ENDEAVOR	18 FEB	1459Z	COLD SIDE	50 KM
OCEANUS	18 FEB	1525Z	WARM SIDE	
ENDEAVOR	21 FEB	1952Z	WARM SIDE	89 KM
OCEANUS	21 FEB	1915Z	COLD SIDE	
ENDEAVOR	5 MAR	0616Z	COLD SIDE	22 KM
OCEANUS	5 MAR	0542Z	WARM SIDE	
ENDEAVOR	5 MAR	2054Z	WARM SIDE	54 KM
OCEANUS	5 MAR	1952Z	COLD SIDE	
ENDEAVOR	6 MAR	1226Z	COLD SIDE	239 KM
OCEANUS	6 MAR	1151Z	WARM SIDE	
ENDEAVOR	7 MAR	0014Z	COLD SIDE	276 KM
OCEANUS	7 MAR	0011Z	WARM SIDE	
ENDEAVOR	22 FEB	1919Z	WARM SIDE	46 KM
OCEANUS	22 FEB	1825Z	WARM SIDE	
ENDEAVOR	24 FEB	1413Z	WARM SIDE	37 KM
OCEANUS	24 FEB	1358Z	WARM SIDE	
ENDEAVOR	27 FEB	2357Z	WARM SIDE	174 KM
OCEANUS	28 FEB	0016Z	WARM SIDE	
ENDEAVOR	5 MAR	0014Z	WARM SIDE	9 KM
OCEANUS	4 MAR	2348Z	WARM SIDE	
ENDEAVOR	7 MAR	0606Z	WARM SIDE	331 KM
OCEANUS	7 MAR	0551Z	WARM SIDE	
ENDEAVOR	19 FEB	1200Z	COLD SIDE	37 KM
OCEANUS	19 FEB	1215Z	COLD SIDE	

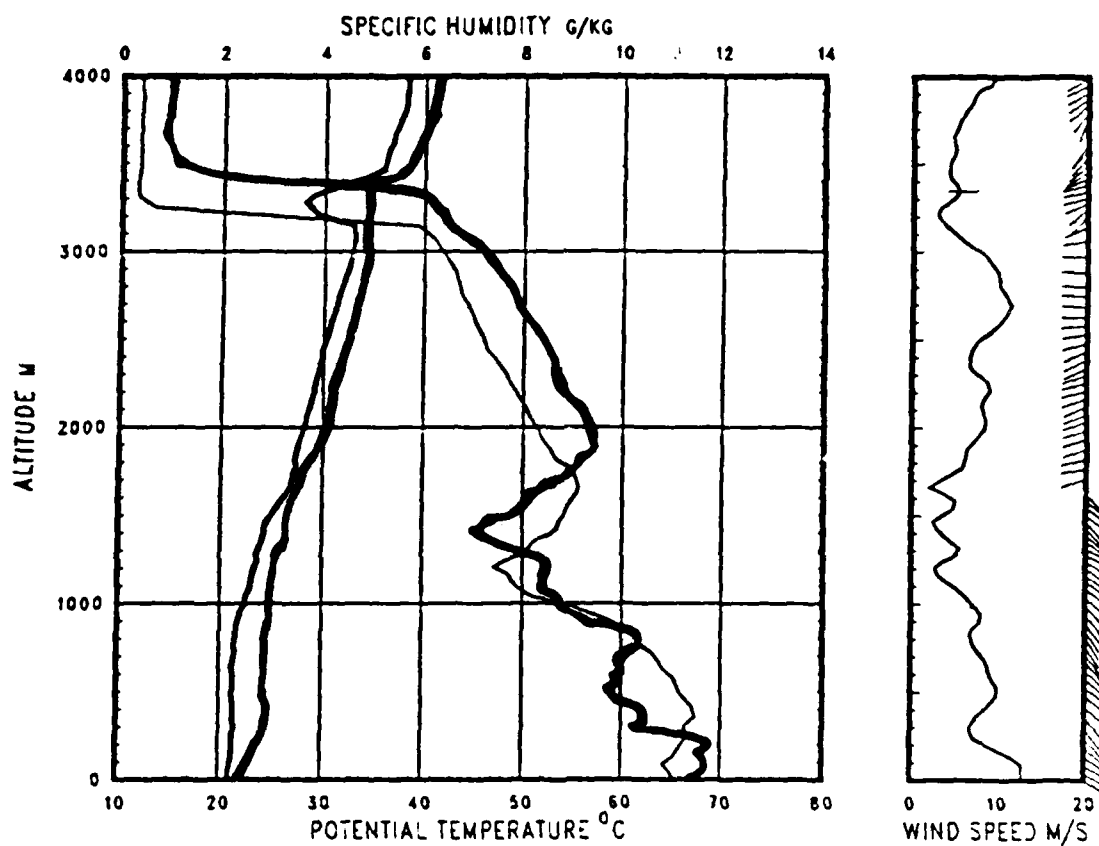


Figure 3.25 Radiosonde Profile Comparison  
 ENDEAVOR 17 Feb. 86, 2352 GMT, 28 18N, 70 25W, cold side (thin).  
 OCEANUS 18 Feb. 86, 0049 GMT, 28 02N, 70 05W, warm side (thick).

A second set of soundings taken on 18 February at 1459 GMT and 1521 GMT were also from opposite sides of the oceanic front. ENDEAVOR was on the cold side, OCEANUS was on the warm and the ship separation distance was 50 km. Wind direction at sea-level was from the south-southeast and changed to south-southwest at the top of the mixed layer. Wind direction across the front was from the warm side to the cold side. The two profiles are similar to the first set of soundings in that the warm side mixed layer depth was higher by 250 m (Fig. 3.26). Both profiles are well mixed to the inversion and similar in shape. The warm side specific humidity is more moist, with the exception of a small layer at 1200-1400 m (just above the inversion). Wind speed at sea-level was  $9 \text{ ms}^{-1}$  and increased slightly to  $10 \text{ ms}^{-1}$  at the top of the mixed layer.

The upper-level trough deepened and moved out of the FASINEX area on 21 February. Sea-level pressure increased and wind speed was  $4 \text{ ms}^{-1}$  from the northeast. Rawinsonde sounding pairs taken at 1915 GMT and 1952 GMT were from opposite sides of the oceanic front. ENDEAVOR was on the warm side, OCEANUS on the cold. The ships were 89 km apart. Wind direction across the front was from the cold side to the warm side with a low-level jet present from 100-500 m which reached a wind speed max of  $15 \text{ ms}^{-1}$ . An interesting feature noted in these profiles is the cold side mixed layer height is higher than the warm side by about 400

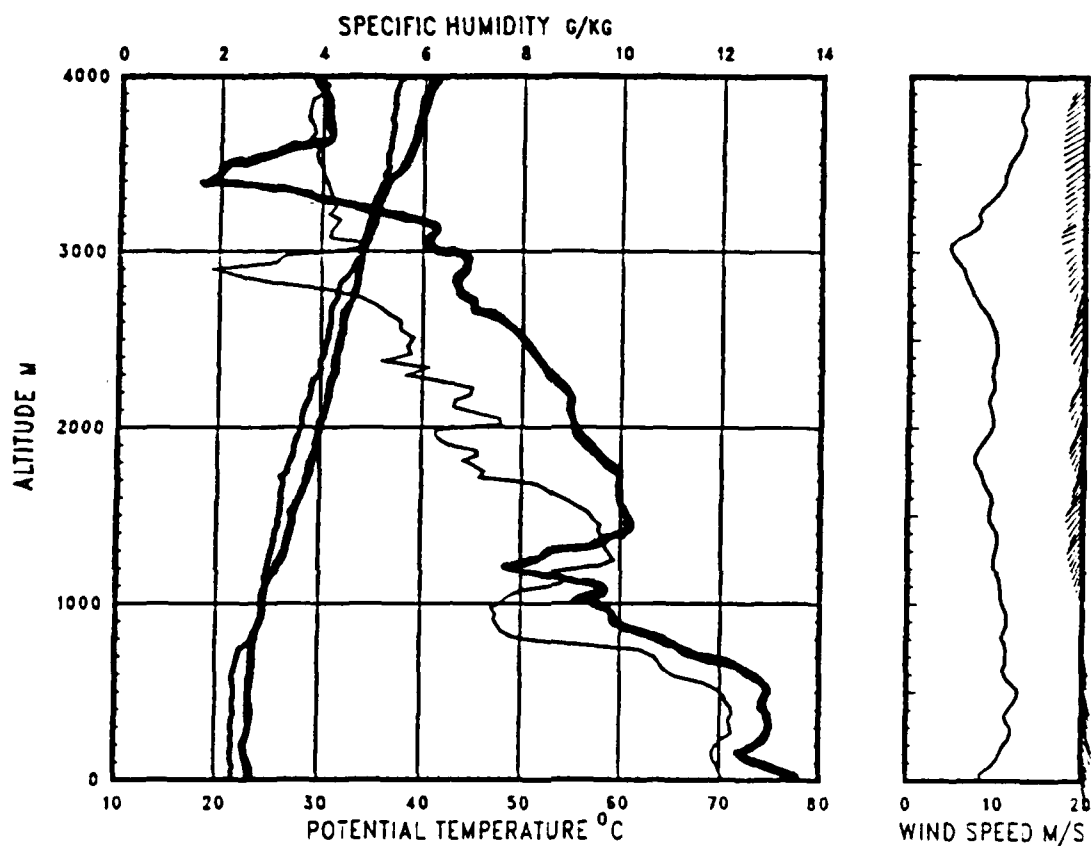


Figure 3.26 Radiosonde Profile Comparison  
 ENDEAVOR 18 Feb. 86, 1459 GMT, 28 28N, 70 29W, cold side (thin).  
 OCEANUS 18 Feb. 86, 1525 GMT, 28 04N, 70 15W, warm side (thick).

m (Fig. 3.27). A secondary inversion on the warm side profile is higher than the cold side by about 400 m, otherwise the potential temperature profiles are quite similar. The specific humidity profiles are very similar with the warm side being more moist from sea-level to 600 m (top of mixed layer) and the cold side more moist from 600-4000 m.

A deepening upper-level trough steered a low pressure system into the FASINEX area bringing in a cold front on 5 March. Sea-level pressure decreased and wind speed was  $14 \text{ ms}^{-1}$  from the northwest. Rawinsonde launch pairs were made at 0542 GMT and 0616 GMT on opposite sides of the front. ENDEAVOR was on the cold side, OCEANUS on the warm. The ships were 22 km apart. Soundings were obtained at 0542 GMT and 0616 GMT on opposite sides of the front. The potential temperature profiles are nearly exact, the difference being the warmer side mixed layer is higher by 700 m, and in a small layer from 1300-1800 m where the cold side potential temperature is higher (Fig. 3.28). Although both specific humidity profiles are equal at sea-level, at 200-1500 m the cold side specific humidity was more moist. From 1500-1900 m the warm side is more moist. Overall the two profiles are quite similar. The wind direction was parallel to the front during these launches.

A second pair of rawinsonde launches on 5 March at 1952 GMT and 2054 GMT were also from opposite sides of the

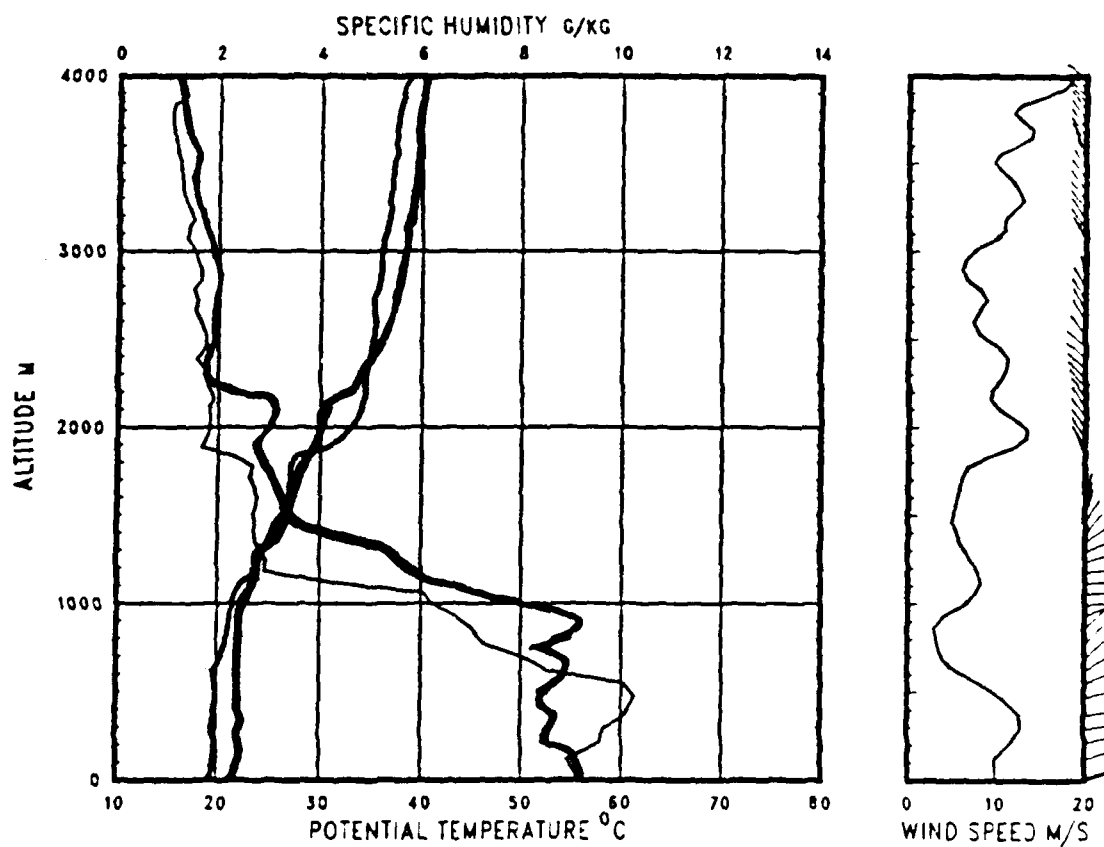


Figure 3.27 Radiosonde Profile Comparison  
 ENDEAVOR 21 Feb. 86, 1952 GMT, 28 12N, 70 03W, warm side (thin).  
 OCEANUS 21 Feb. 86, 1915 GMT, 28 59N, 69 56W, cold side (thick).



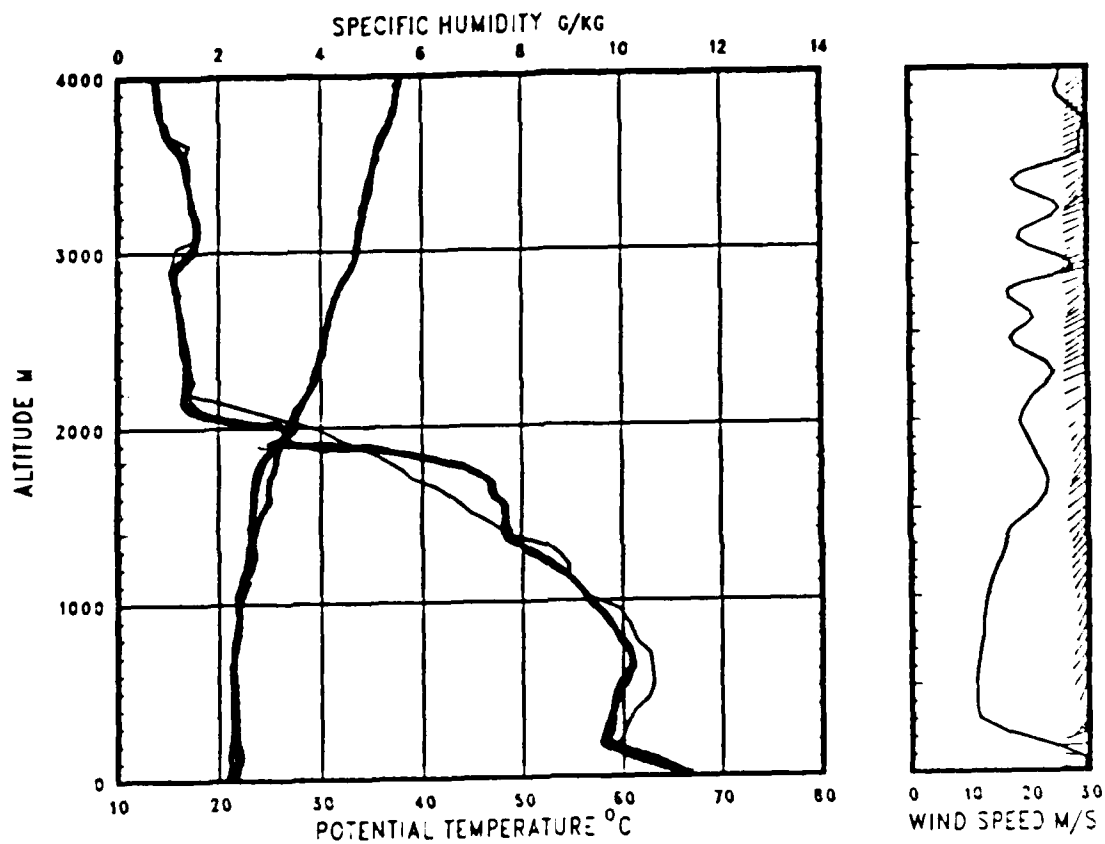


Figure 3.28 Radiosonde Profile Comparison  
 ENDEAVOR 05 Mar. 86, 0616 GMT, 28 53N, 67 52W, cold side (thin).  
 OCEANUS 05 Mar. 86, 0542 GMT, 28 46, 68 03W, warm side (thick).

oceanic front, with ENDEAVOR on the warm side and OCEANUS on the cold separated by 54 km. Wind direction across the front was from the warm side to the cold side. The mixed layer depths here are approximately equal with the warm side potential temperature just slightly warmer than the cold side. Overall, the two profiles are identical being well mixed below the inversion. The cold side specific humidity is much more moist at sea-level ( $11 \text{ gkg}^{-1}$ ) than the warm side ( $9 \text{ gkg}^{-1}$ ). This condition extends to 400 m where the warm side specific humidity becomes more moist to the top of the mixed layer (Fig. 3.29). From 1500-2300 m the cold side profile was more moist and from 2300-4000 m the specific humidity profiles become similar.

On 6 March the upper-level trough and surface frontal system had passed through the FASINEX area by 1000 GMT. Sea-level pressure began to increase and wind speed was negligible. The sounding pair taken at 1151 GMT and 1226 GMT are from opposite sides of the front, with ENDEAVOR on the cold side and OCEANUS on the warm side 239 km apart. Wind direction across the front is from the cold side to the warm side. The mixed layer depths are again nearly similar (Fig. 3.30). The warm side potential temperature is, at all levels, higher than the cold side. Both profiles are quite similar and well mixed below the inversion. The warm side specific humidity profile is more moist from sea-level to 500 m. From 500-1500 m the cold side profile became more

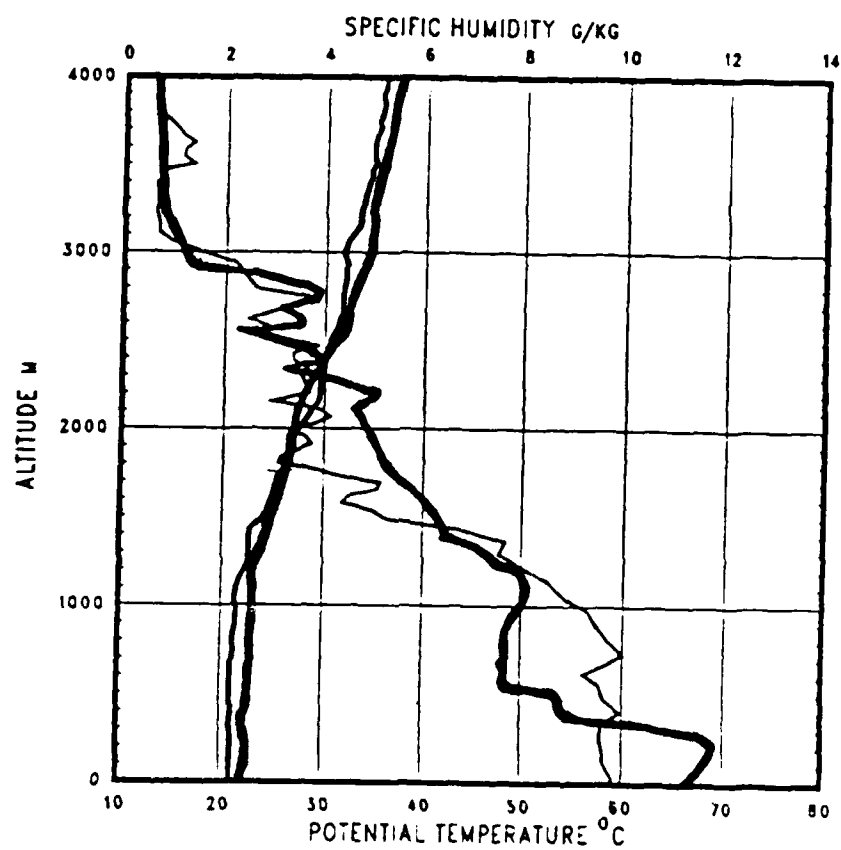


Figure 3.29 Radiosonde Profile Comparison  
 ENDEAVOR 05 Mar. 86, 2054 GMT, 28.45N, 67.47W, warm side (thin).  
 OCEANUS 05 Mar. 86, 1952 GMT, 29.14N, 67.50W, cold side (thick).

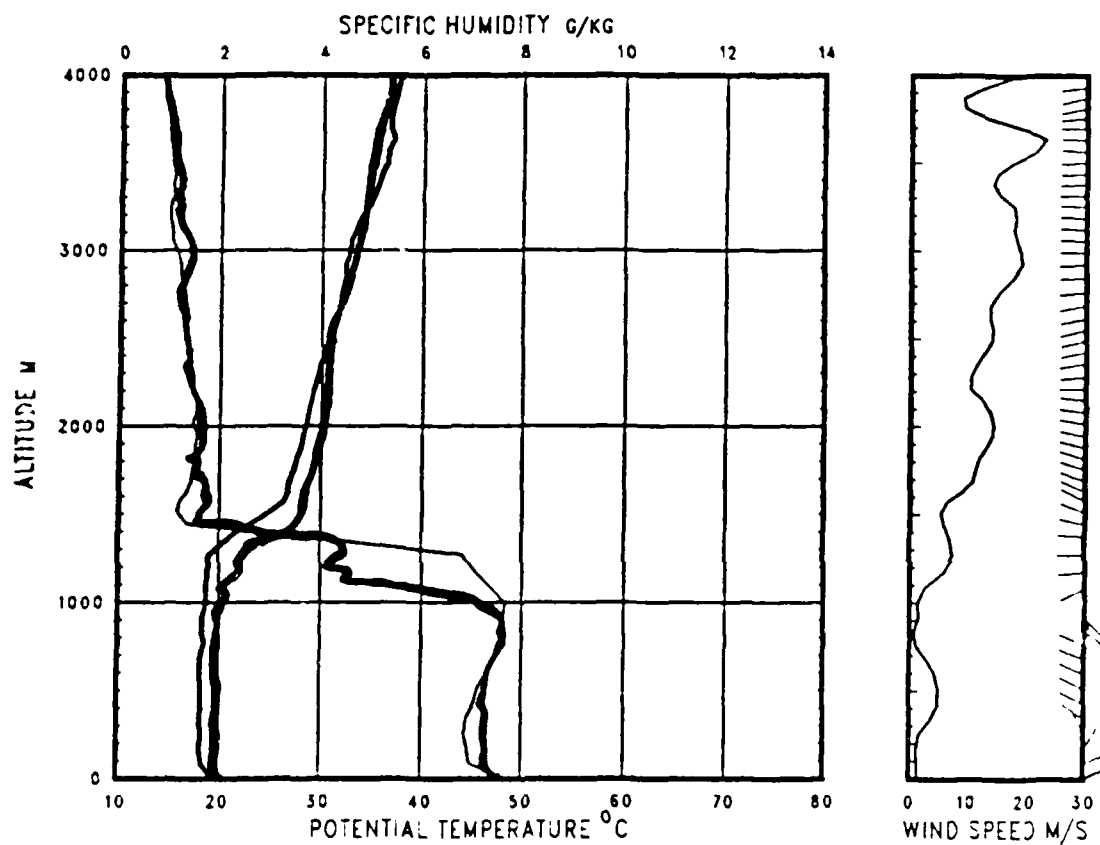


Figure 3.30 Radiosonde Profile Comparison  
 ENDEAVOR 06 Mar. 86, 1226 GMT, 28 50N, 67 36W, cold side (thin),  
 OCEANUS 06 Mar. 86, 1151 GMT, 27 17N, 69 17W, warm side (thick).

moist. Above 1500 m the specific humidity profiles are very similar.

An upper-level trough and sea-level low pressure system developed on 7 March. Sea-level pressure was 1041-1016 mb and wind speed was  $4-10 \text{ ms}^{-1}$  from the southwest. Sounding pairs taken at 0011 GMT and 0014 GMT are from opposite sides of the front, ENDEAVOR on the cold side and OCEANUS on the warm side 276 km apart. Wind direction across the front was from the warm side to the cold side with a low level jet present from 200-800 m reaching a wind speed max of  $20 \text{ ms}^{-1}$ . Both potential temperature profiles are identical from sea-level to 1200 m. The cold side mixed layer depth is slightly higher than the warm side. Above the mixed layer the cold side potential temperature is higher. The cold side specific humidity profile is drier than the warm side from the sea-level to 800 m (Fig. 3.31). From 800-1600 m the warm side becomes drier. A large specific humidity difference is noted 1600-3000 m where the warm side becomes very moist and the cold side very dry. Specific humidity profiles are dissimilar above the mixed layer.

Conditions were dominated by an upper-level ridge and associated subtropical high on 22 February. Sea-level pressure was 1013-1016 mb and wind speed was negligible. Rawinsonde launches occurred at 1825 GMT and 1919 GMT from the warm side of the front, with the ships 46 km apart.

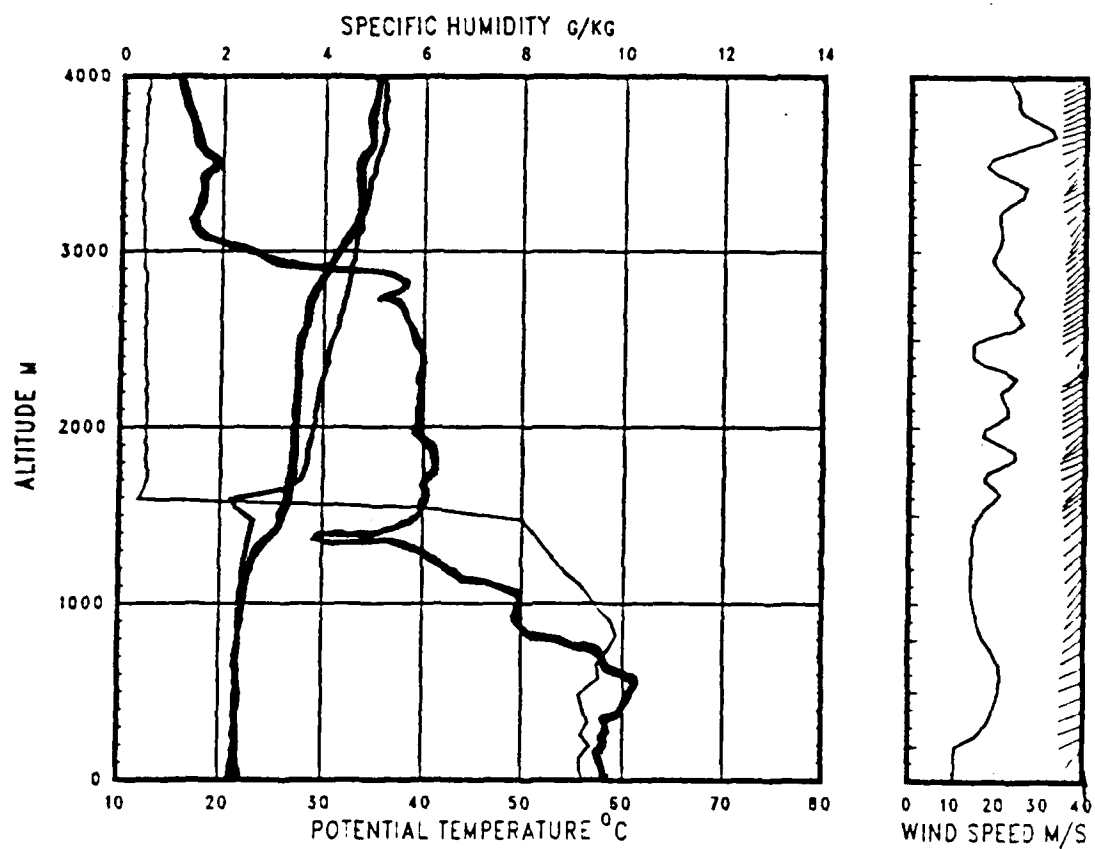


Figure 3.31 Radiosonde Profile Comparison  
ENDEAVOR 07 Mar. 86, 0014 GMT, 28 36N, 67 18W, cold side (thin).  
OCEANUS 07 Mar. 86, 0011 GMT, 27 08N, 69 34W, warm side (thick).

Potential temperature profiles both taken on the warm side of the front are identical in all respects. Mixed layer depth is 1200 m and both profiles are well mixed below the inversion (Fig. 3.32). The specific humidity profiles are similar except the ENDEAVOR's sounding is more moist from sea-level to 500 m and OCEANUS's sounding is more moist from 500 m and above.

A cold front had stalled west of the FASINEX area on 24 February. Sea-level pressure dropped slightly and wind speed was  $5-8 \text{ ms}^{-1}$  from the southwest. The rawinsonde sounding pair taken at 1358 GMT and 1413 GMT are from the warm side of the front, with a ship separation distance of 37 km. The potential temperature profiles are identical up to 1000 m. Mixed layer depth differed by approximately 300 m (Fig. 3.33). Oceanus's potential temperature is slightly higher from 1000-2000 m. The specific humidity profiles are also very similar with ENDEAVOR's sounding being more moist to the top of the mixed layer and OCEANUS's being more moist above the mixed layer.

On 27 and 28 February a low pressure system was dominating the synoptic-scale situation. Sea-level pressure was 1013-1015 mb and wind speed was  $8-10 \text{ ms}^{-1}$  from the southwest. The rawinsonde launches at 2357 GMT 27 February and 0016 GMT 28 February were from the warm side of the oceanic front. The ships were 174 km apart. Potential temperature and specific humidity profiles are almost

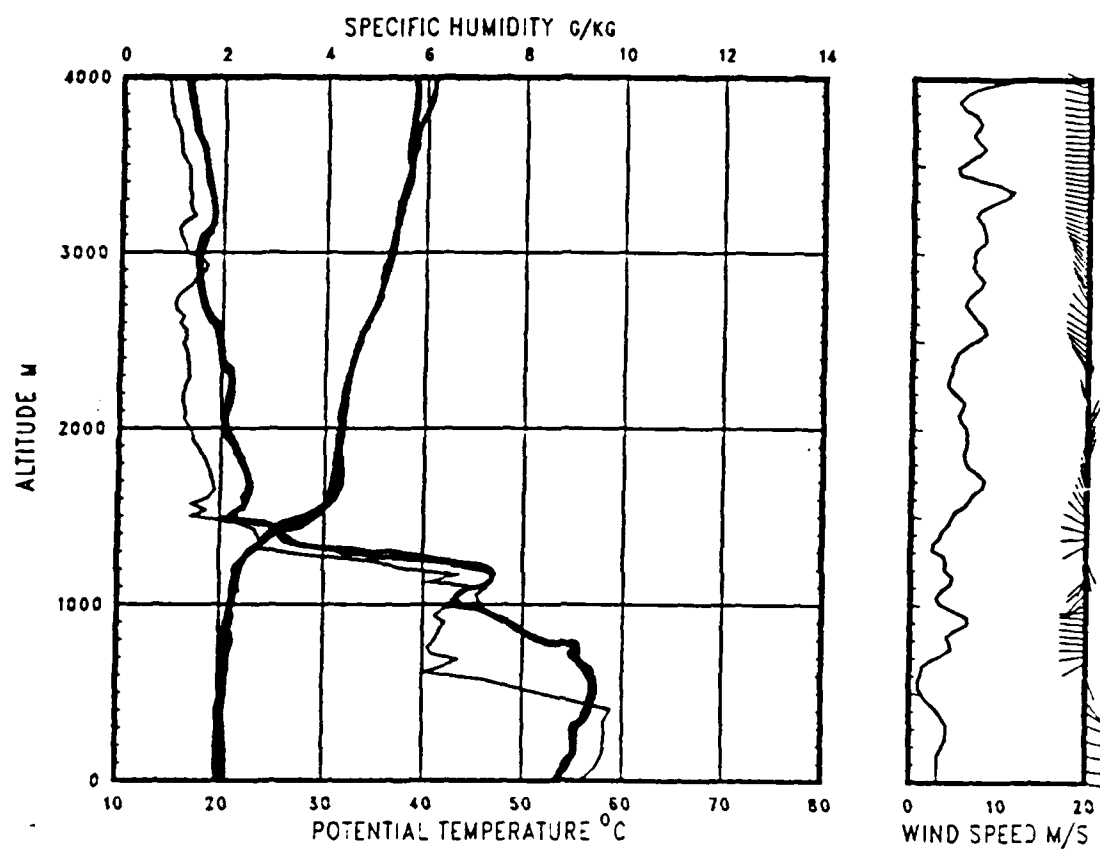


Figure 3.32 Radiosonde Profile Comparison  
ENDEAVOR 22 Feb. 86, 1919 GMT, 28 18N, 69 20W, warm side (thin).  
OCEANUS 22 Feb. 86, 1825 GMT, 28 13N, 69 48W, warm side (thick).



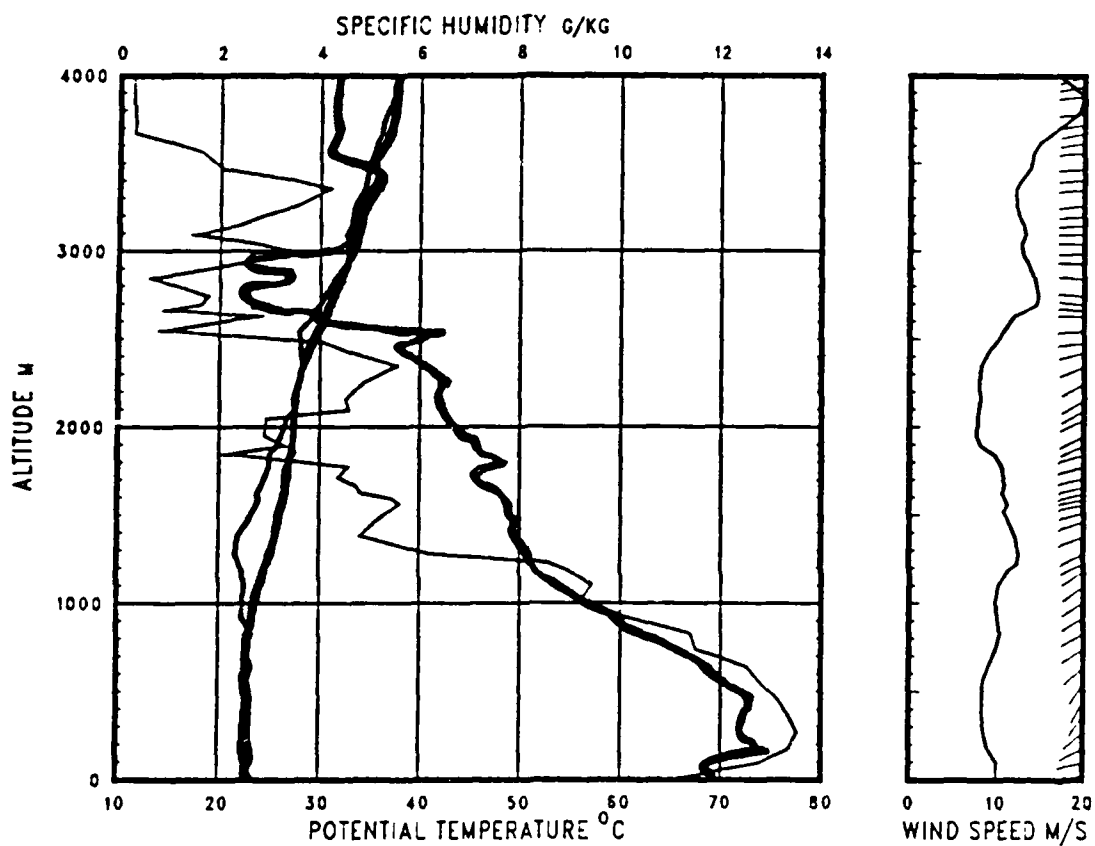


Figure 3.33 Radiosonde Profile Comparison  
 ENDEAVOR 24 Feb. 86, 1413 GMT, 27 56N, 69 49W, warm side (thin),  
 OCEANUS 24 Feb. 86, 1358 GMT, 28 14N, 69 40W, warm side (thick).

identical with the OCEANUS mixed layer depth slightly higher and ENDEAVOR's specific humidity profile more moist from 500-1000 m (Fig. 3.34). A second pair of soundings taken at 2348 GMT 4 March and 0014 GMT 5 March from the warm side of the front closely resemble the previously discussed soundings and exhibit the same characteristics (Fig. 3.35).

A second sounding pair on 7 March at 0551 GMT and 0606 GMT had both launches from the warm side of the oceanic front, 331 km apart. OCEANUS's mixed layer depth is lower by 250 m and warmer than that of ENDEAVOR, otherwise the two profiles are very similar (Fig. 3.36). OCEANUS's specific humidity is more moist to the top of the mixed layer and then ENDEAVOR's becomes more moist up to 1900 m. From 1900-2800 m OCEANUS's sounding again becomes more moist. Overall the specific humidity profiles are not very similar.

On 19 February an upper-level trough and sea-level low pressure system were present in the FASINEX area. Sea-level pressure was decreasing and wind speed was  $4-6 \text{ ms}^{-1}$  from the southwest. Rawinsonde sounding pairs taken at 1200 GMT and 1215 GMT were both from the cold side of the oceanic front, with the ships 37 km apart. The potential temperature profiles are very similar with ENDEAVOR's mixed layer depth being approximately 300 m lower than OCEANUS's (Fig. 3.37). ENDEAVOR's specific humidity profile is more moist up to 300 m after which both profiles were similar to

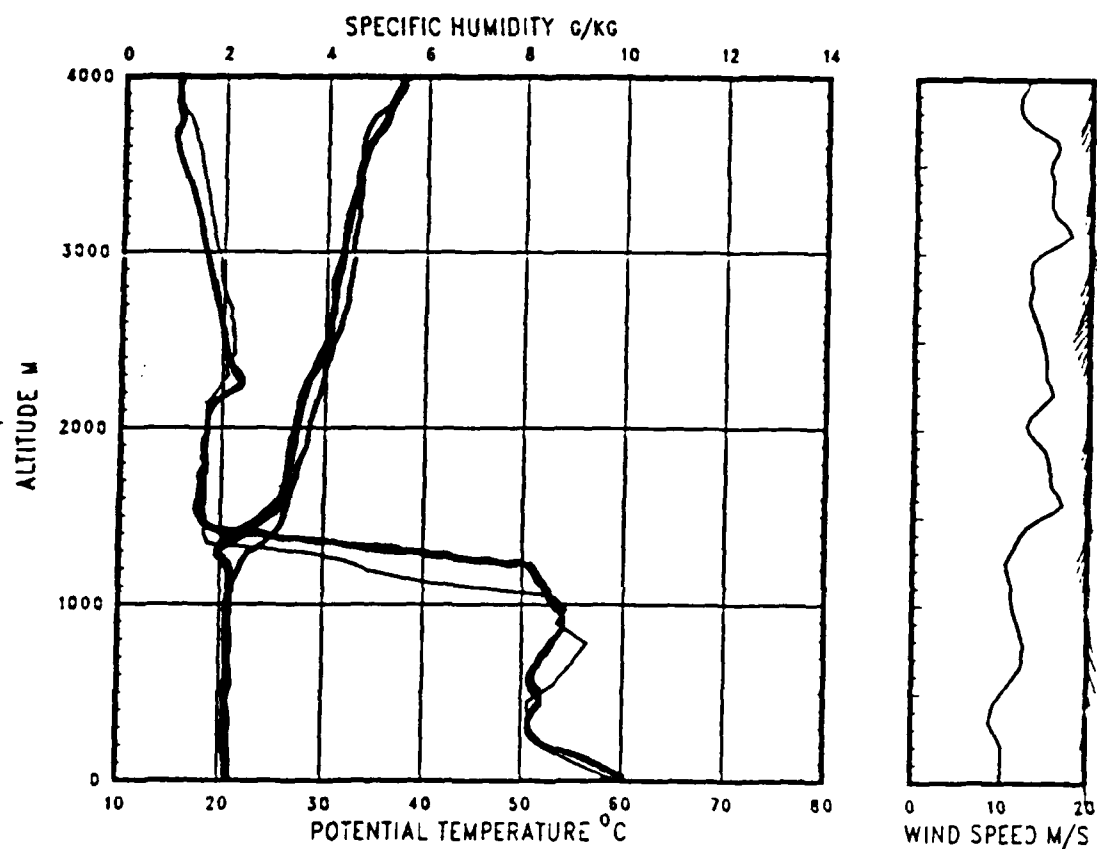


Figure 3.34 Radiosonde Profile Comparison  
 ENDEAVOR 27 Feb. 86, 2357 GMT, 27 10N, 69 48W, warm side (thin).  
 OCEANUS 28 Feb. 86, 0016 GMT, 28 42N, 70 08W, warm side (thick).

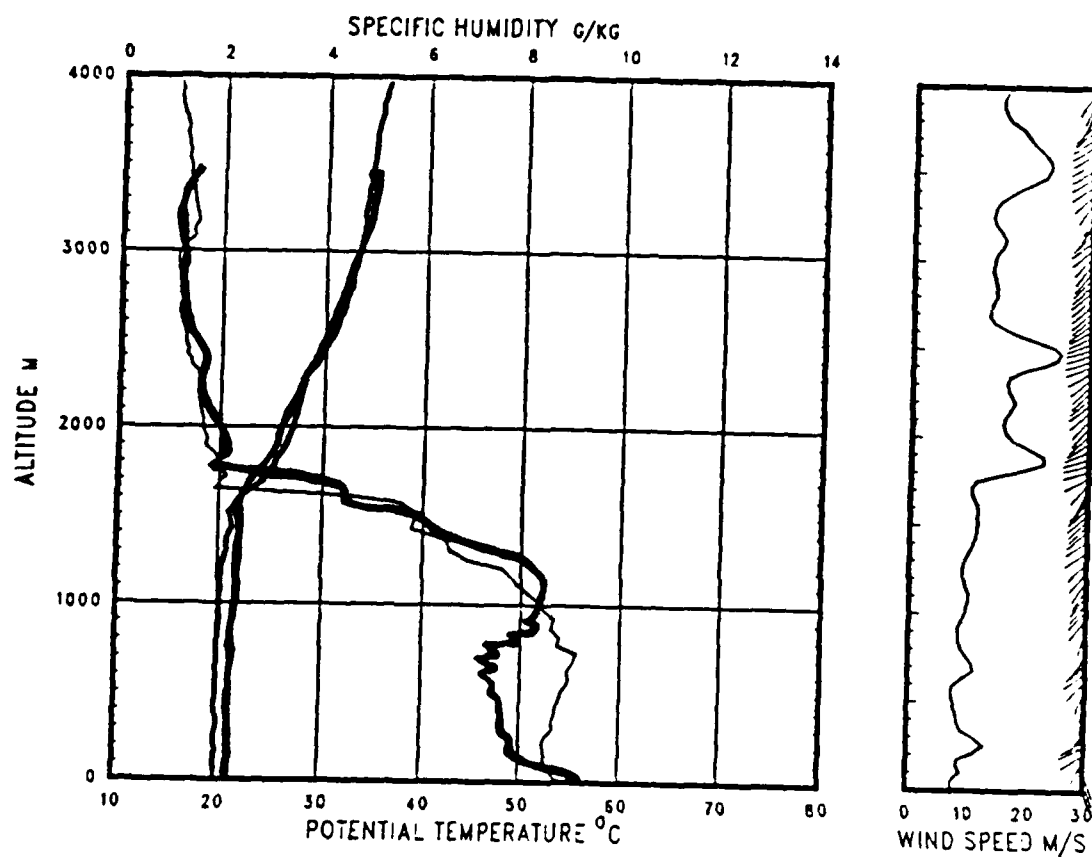


Figure 3.35 Radiosonde Profile Comparison  
ENDEAVOR 05 Mar. 86, 0014 GMT, 28 30N, 68 03W, warm side (thin),  
OCEANUS 04 Mar. 86, 2348 GMT, 28 33N, 68 08W, warm side (thick).

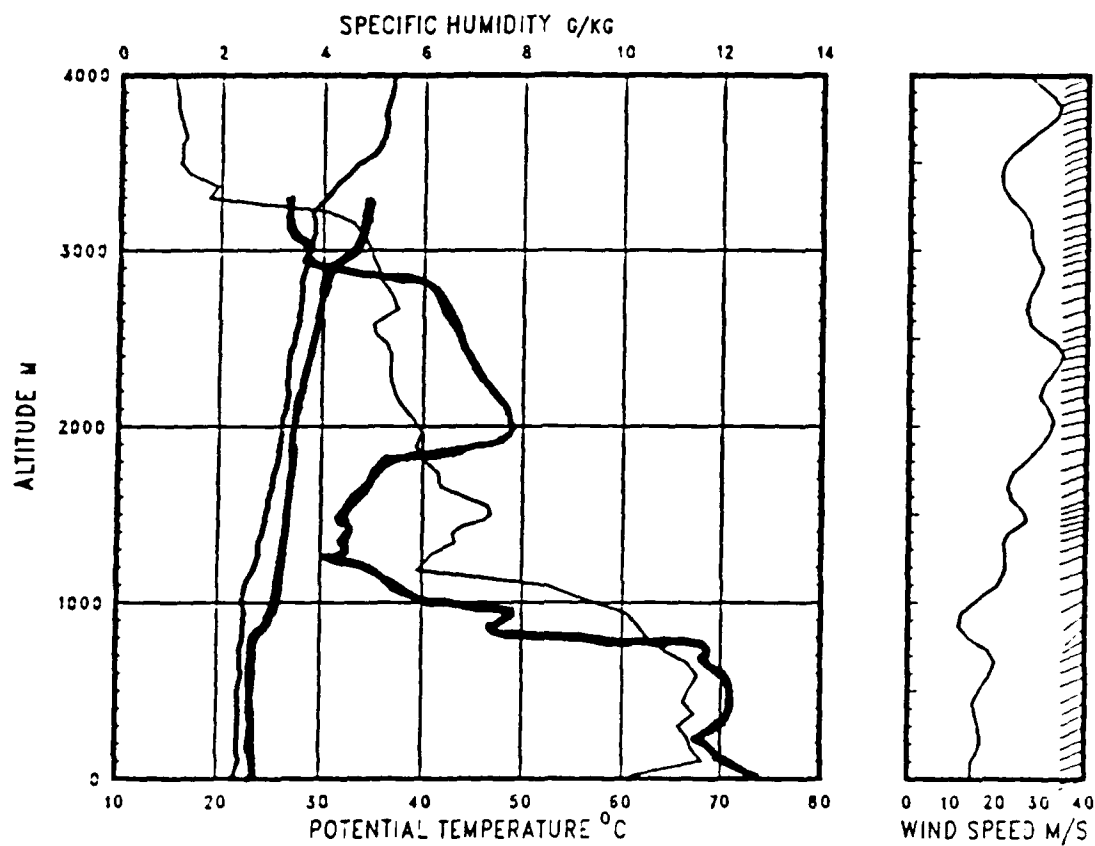


Figure 3.36 Radiosonde Profile Comparison  
 ENDEAVOR 07 Mar. 86, 0606 GMT, 28 50N, 67 28W, warm side (thin).  
 OCEANUS 07 Mar. 86, 0551 GMT, 26 54N, 70 02W , warm side (thick).

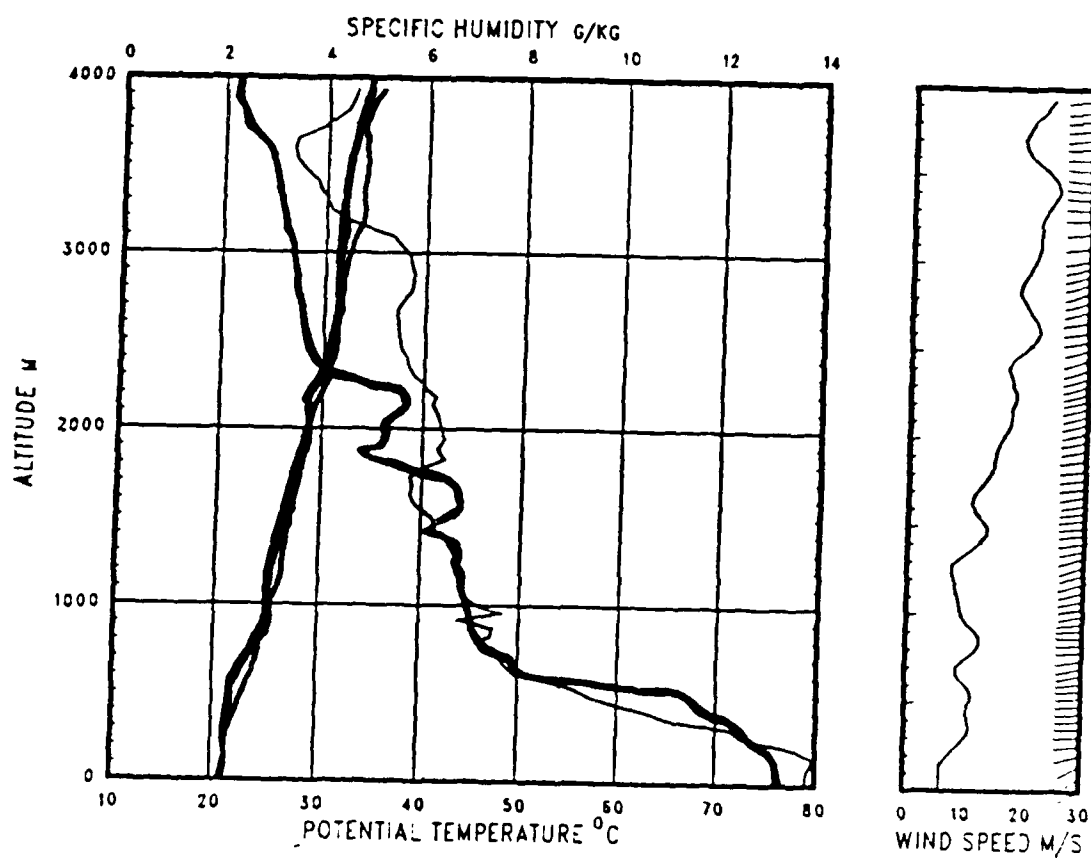


Figure 3.37 Radiosonde Profile Comparison  
 ENDEAVOR 19 Feb. 86, 1200 GMT, 28 47N, 70 11W, cold side (thin).  
 OCEANUS 19 Feb. 86, 1215 GMT, 28 49N, 70 34W, cold side (thick).

1800 m. Above 1800 m OCEANUS's specific humidity was noticeably drier.

#### IV. SUMMARY AND CONCLUSIONS

FASINEX was planned and designed to gain an understanding of coupled changes in adjacent atmospheric and ocean mixed layers in the vicinity of a subtropical sea surface temperature (SST) front. Differences in boundary layer height and mixed layer were expected to occur across the front, however the temporal variation of atmospheric synoptic scale systems transiting the FASINEX area led to including near simultaneous rawinsonde launches from separated ships to characterize both spatial as well as temporal variation of the MABL. The data did indeed show that temporal changes over periods of 12 to 18 hours were dominant in local variations. MABL variations observed in FASINEX were described in this thesis in terms of temporal variations relative to the synoptic-scale features and spatial variations relative to the SST fronts.

Significant changes in the synoptic-scale features and flow pattern occurred throughout the 14 February to 9 March FASINEX period. For every three-day period there is a change in synoptic features affecting the MABL. These changes were associated with low pressure systems moving west to east off the eastern U.S. coast between 30°N and 35°N.

The associated trough (front) passages and changes in low-level and upper-level advection affected the MABL in the FASINEX area. During these periods MABL features exhibited



those due to larger scale convergence and the effect of sea-level conditions were masked.

Between the transiting low pressure systems, occurring every three days, conditions associated with intensification of the subtropical anticyclone or passage of the post frontal anticyclone affected the MABL. Because these anticyclonic influenced periods lasted two days, at most, the MABL was always evolving due to changes in the synoptic-scale forcing even with non-disturbed conditions.

Primary MABL changes that occurred within anticyclone influences in association with synoptic-scale forcing, were increases or decreases in mixed layer temperature and specific humidity. Examination of wind direction relative to the front and changes in mixed layer potential temperature and specific humidity on either side of the front suggests these effects are caused by advection from upwind cold or warm sea-level temperature areas. This also suggests that the depth of the mixed layer is not highly correlated with expected advection or to variations of the subsidence rates. Height variation of the vector wind were quite pronounced, suggesting differential advection was important to changes of both temperature and humidity across the inversion.

MABL variations due to the SST front were examined within different synoptic-scale conditions. Thirteen pairs were examined which included rawinsonde comparisons with the

MABL variations due to the SST front were examined within different synoptic-scale conditions. Thirteen pairs were examined which included rawinsonde comparisons with the ships on opposite sides (7 pairs) of the front as well as on the same side (6 pairs) of the front. Inspection of the radiosonde profiles showed differences (mixed layer height, potential temperature and specific humidity) between paired soundings were clearly larger when rawinsondes were from opposite sides of the front. Flow direction across the front did not appear to be an important factor in the differences.

The primary differences in rawinsondes from opposite sides of the front is an increase in the occurrence height of features in potential temperature on the warm side of the front of 200-300 meters. These include the height of the moist (turbulent layer) as well as the height of layers with maximum or minimum specific humidity.

Even though MABL features were observed with simultaneous spatially separated rawinsonde launches combination of both shipboard and aircraft data was necessary for physically complete descriptions of the front effect. The primary contribution to the descriptions obtained from the shipboard data was the establishment of the synoptic scale and the indication of SST front effects.

AD-A184 006

PROPERTIES OF THE ATMOSPHERIC BOUNDARY LAYER ABOVE A  
SUBTROPICAL OCEANIC FRONT(U) NAVAL POSTGRADUATE SCHOOL  
MONTEREY CA J P HIGGINS JUN 87

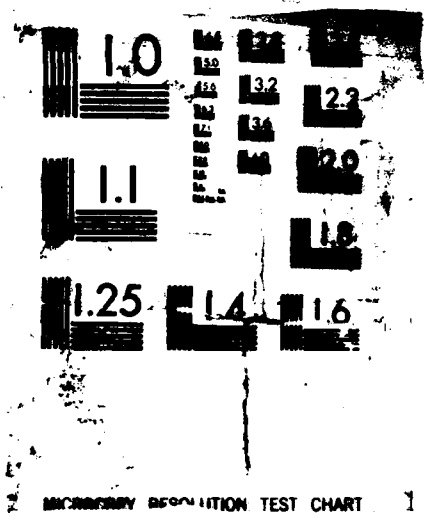
2/2

UNCLASSIFIED

F/G 4/2

NL





RESOLUTION TEST CHART 1

# LIST OF REFERENCES

- Businger, J. A., 1985: The marine boundary layer from air-sea interface to inversion. NCAR/TN-252+STR, National Center for Atmospheric Research. Boulder, Co., 84 pp.
- Businger, J. A., Shaw, W. J., 1984: The response of the marine boundary layer to mesoscale variations in sea-surface temperature. *Dynamics of Atmospheres and Oceans*, 8, 267-281.
- Department of Transportation, U.S. Coast Guard, COMDTINST M16562.3, *Loran C User Handbook*, 63 pp.
- Davidson, K. L., C. W. Fairall, P. J. Boyle, and G. E. Schacher, 1984: Verification of an atmospheric mixed-layer model for a coastal region. *J. Clim. Appl. Meteor.*, 23, 617-636.
- Hsu, S. A., Fett, R., and P. E. La Violette, 1985: Variations in atmospheric mixing height across oceanic thermal fronts. *J. Geo. Res.*, 90, 3211-3224.
- Randall, D. A., 1979: Entrainment into a stratocumulus layer with distributive radiative cooling. *J. Atmos. Sci.*, 37, 148-159.
- Stage, S. A., Weller, R. A., 1985: The frontal air-sea interaction experiment (FASINEX); Part I: Background and scientific objectives. *Bulletin of the Amer. Met. Soc.*, 66, 1511-1520.
- Weller, R. A., Stage, S. A., 1984: *FASINEX (Frontal Air-Sea Interaction Experiment) scientific program and field plan, Vol 1*. Woods Hole Oceanographic Institute, Woods Hole, Ma. 02543, 100 pp.
- Wyngaard, J. C., 1984: Structure of the planetary boundary layer and implications for its modelling. *National Center for Atmospheric Research*, Boulder, Co., 35 pp.
- Wyngaard, J.C., Brost, R.A., 1983: Top-down and bottom-up diffusion of a Scalar in the Convective Boundary Layer. *J. Atmos. Sci.* 41, 102-112.

# INITIAL DISTRIBUTION LIST

	No.	Copies
1. Defense Technical Information Center Cameron Station Alexandria, VA 22304-6145	2	
2. Library, Code 0142 Naval Postgraduate School Monterey, CA 93943-5002	2	
3. Chairman, Code 68Tm Department of Oceanography Naval Postgraduate School Monterey, CA 93943-5000	1	
4. Chairman, Code 63Rd Department of Meteorology Naval Postgraduate School Monterey, CA 93943-5000	1	
5. Professor K.L. Davidson, Code 63Ds Department of Meteorology Naval Postgraduate School Monterey, CA 93943-5000	5	
6. Professor W.J. Shaw, Code 63Sr Department of Meteorology Naval Postgraduate School Monterey, CA 93943-5000	1	
7. LT. John P. Higgins 6 Arlene St.. Brockton, MA 02402	1	
8. Director Naval Oceanography Division Naval Observatory 34th and Massachusetts Avenue NW Washington, DC 20390	1	
9. Commander Naval Oceanography Command NSTL Station Bay St. Louis, MS 39522	1	
10. Commanding Officer Naval Oceanographic Office NSTL Station Bay St. Louis, MS 39522	1	

11. Commanding Officer 1  
Fleet Numerical Oceanography Center  
Monterey, CA 93943
12. Commanding Officer 1  
Naval Ocean Research and Development  
Activity  
NSTL Station  
Bay St. Louis, MS 39522
13. Commanding Officer 1  
Naval Environmental Prediction  
Research Facility  
Monterey, CA 93943
14. Chairman, Oceanography Department 1  
U.S. Naval Academy  
Annapolis, MD 21402
15. Chief of Naval Research 1  
800 N. Quincy Street  
Arlington, VA 22217
16. Office of Naval Research, Code 420 1  
Naval Ocean Research and Development  
Activity  
800 N. Quincy Street  
Arlington, VA 22217
17. Commander 1  
Oceanographic Systems Pacific  
Box 1390  
Pearl Harbor, HI 96860
18. Commander, Air-370 1  
Naval Air Systems Command  
Washington, DC 20360
19. Chief, Ocean Services Division 1  
National Oceanic and Atmospheric  
Administration  
8060 Thirteenth Street  
Silver Springs, MD 20910
20. Commanding Officer 1  
Naval Eastern Oceanography Center  
Naval Air Station  
Norfolk, VA 23511

END

10-81

DTIC